Recent single Higgs measurements with the ATLAS detector

Lailin Xu

University of Sci. & Tech. of China

On behalf of the ATLAS Collaboration

Moriond EW 2026

2026.3.15-22, La Thuile

Introduction

- The Higgs boson is essential in the Electroweak Symmetry Breaking
- Great progress made in *theory/experiment* to deepen our understanding
- Current knowledge of the Higgs boson motivates further characterization to have a full picture
- The Higgs boson also provides an important portal to probe new physics

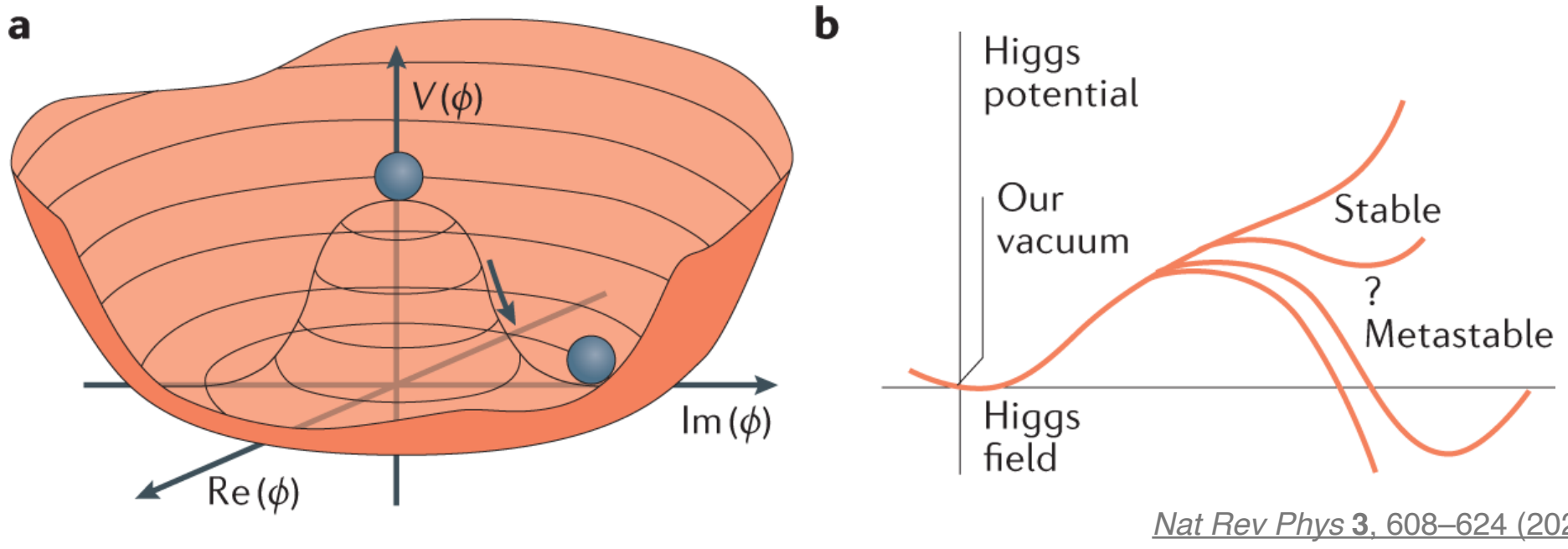

Nat Rev Phys **3**, 608–624 (2021)

Latest single-Higgs measurements from ATLAS

- **Run2** legacy: 140 fb^{-1} @ 13 TeV
  - Combined CP measurements in HVV couplings HIGP-2024-26
- **Run3**: 2022-24 data with 164 fb^{-1} @ 13.6 TeV
  - CP and polarization study in VBF H→$\gamma\gamma$ HIGP-2024-23
  - Simplified Template Cross-sections (STXS) and differential measurements in H→4l ATLAS-CONF-2026-003

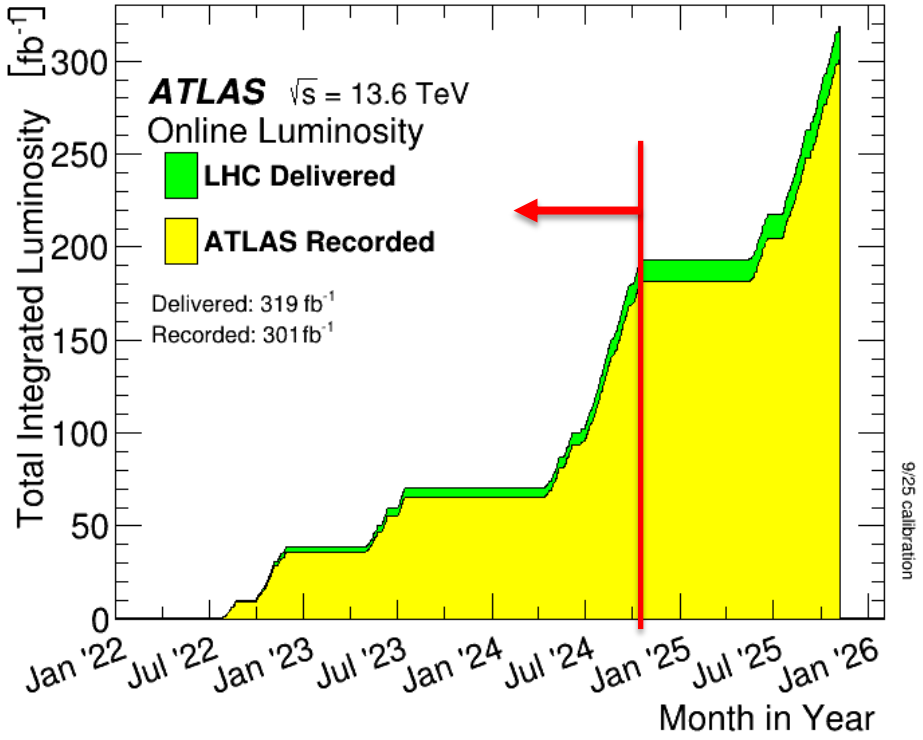

link

Other new results but not covered in this talk:

- First evidence of boosted All-Had Hbb with Run 2+Run 3, HIGP-2024-01
- Run2 tH combination, ATLAS-CONF-2026-002

See Gaetano Barone's talk and also the backup

Run2 legacy: HVV CP combination

HIGP-2024-26

CP properties of Higgs couplings

- ***Big question**: What's the origin of matter-antimatter asymmetry of the Universe?*
- Sakharov conditions: additional sources of CP violation beyond the SM are required
- Are there CP-violating Higgs couplings? → Measuring the CP structure of Higgs boson couplings to EWK gauge bosons (HVV) and fermions (Hff)
  - Current experimental sensitivity still allows for possible CP-violating contributions

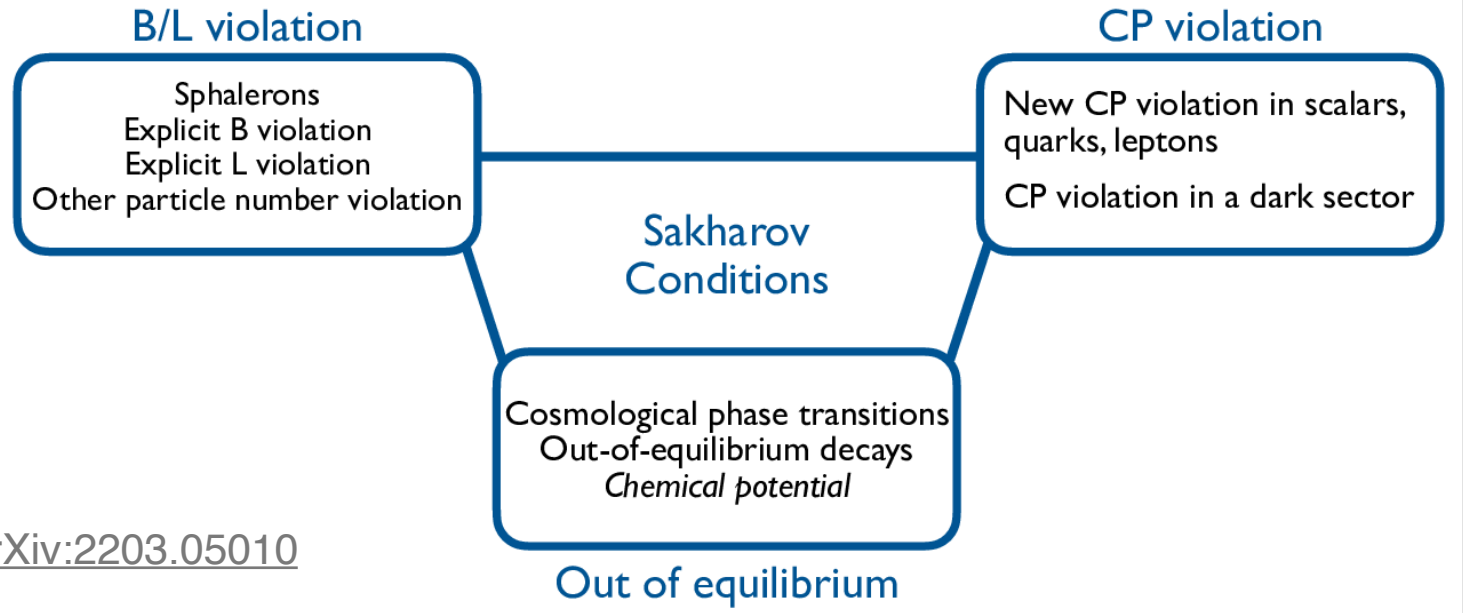

arXiv:2203.05010

ATLAS-CONF-2025-006

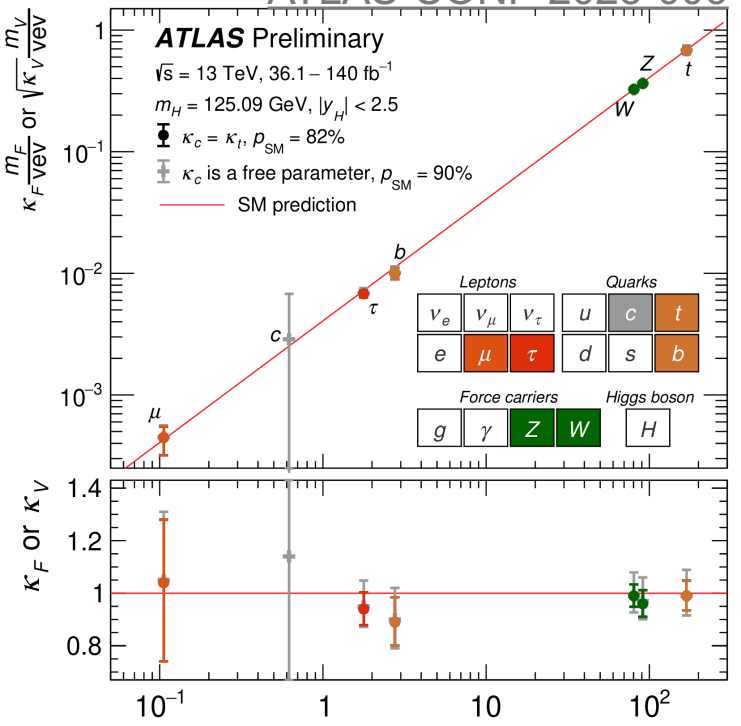

HVV CP

- **HVV couplings** can be probed via VBF/VH production and HVV decays

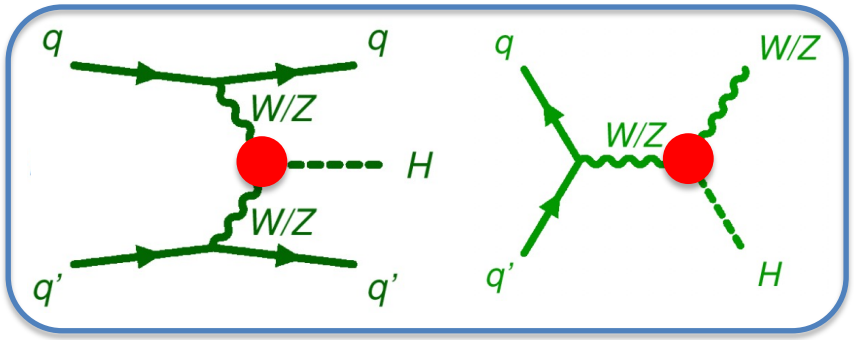

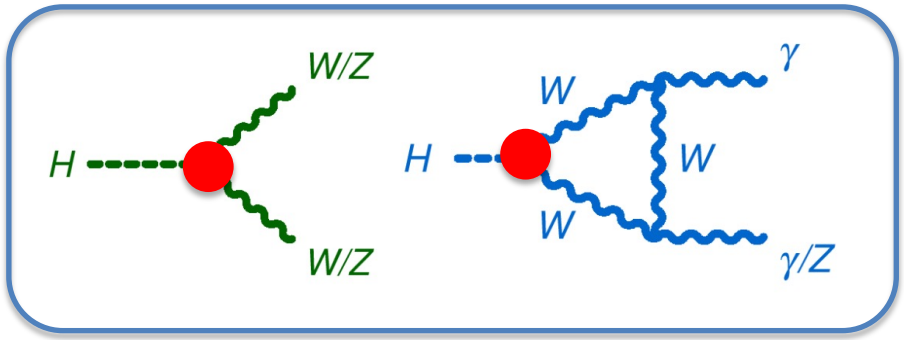

- Using the Standard Model Effective Field Theory (SMEFT) formalism to parameterize the HVV interactions

$$\mathcal{L}_{\text{SMEFT}} = \mathcal{L}_{SM} + \sum_i \frac{c_i}{\lambda^{D-4}} O_i^{(D)}$$

c_i: Wilson coefficients
O_i: SMEFT CP-odd dim-6 operators

Operator	Structure	Coupling
	Warsaw Basis	
$O_{\Phi\tilde{W}}$	$\Phi^\dagger\Phi\tilde{W}^I_{\mu\nu}W^{\mu\nu I}$	$c_{H\widetilde{W}}$
$O_{\Phi\tilde{W}B}$	$\Phi^\dagger\tau^I\Phi\tilde{W}^I_{\mu\nu}B^{\mu\nu}$	$c_{H\widetilde{W}B}$
$O_{\Phi\tilde{B}}$	$\Phi^\dagger\Phi\tilde{B}_{\mu\nu}B^{\mu\nu}$	$c_{H\widetilde{B}}$

Cross-section decomposition:

$$O_n = O_n^{\text{SM}}\left(1 + \sum_i A_{ni}\, c_i + \sum_i B_{ni}\, c_i^2 + \sum_{i<j} C_{nij}\, c_i c_j\right),$$

Linear (CP-odd) | Quadratic (CP-even) | Cross-term (CP-even)

HVV CP combination

HIGP-2024-26

- Dedicated CP measurements have been performed in various production/decay channels, *individually*
- First ATLAS combined measurement of the CP properties of HVV using SMEFT in the Warsaw basis

Input measurements		References	CP observables
Prod.	Decay		
VBF	H→$\gamma\gamma$	PRL 131 (2023) 061802	Optimal Observable(**OO**) shape-only analysis
	H→ZZ*→4l	JHEP 05 (2024) 105	**OO** shape-only analysis
	H→$\tau\tau$	JHEP 10 (2025) 92	**OO** shape-only analysis
	H→WW*→lvlv	EPJC 85 (2025) 1403	$\Delta\boldsymbol{\Phi_{jj}}$ shape-based analysis
WH	H→bb	ATL-PHYS-PUB-2025-022	$\boldsymbol{Q_l \cos\delta^+}$ shape-based analysis

CP-odd OO based on matrix-element ratios

$$OO = \frac{2\mathrm{Re}(\mathcal{M}^*_{\mathrm{SM}}\mathcal{M}_{\mathrm{BSM}})}{|\mathcal{M}_{\mathrm{SM}}|^2}$$

H→ZZ*: sensitive to $c_{H\tilde{B}}, c_{H\tilde{W}B}$

WH: only sensitive to $c_{H\tilde{W}}$

VBF: mainly sensitive to $c_{H\tilde{W}}$, with subleading contributions from $c_{H\tilde{B}}, c_{H\tilde{W}B}$

Q_l: lepton charge

$$\cos\delta^+ = \frac{\mathbf{p}_\ell^{(W)} \cdot (\mathbf{p}_H \times \mathbf{p}_W)}{|\mathbf{p}_\ell^{(W)}| \cdot |\mathbf{p}_H \times \mathbf{p}_W|},$$

Combination strategy

HIGP-2024-26

- Combination strategy:
  - 1D fit: scan $c_{H\widetilde{W}}$ while fixing $c_{H\widetilde{B}} = c_{H\widetilde{W}B} = 0$
  - 3D fit: simultaneously fit $c_{H\widetilde{W}}, c_{H\widetilde{B}}, c_{H\widetilde{W}B}$ → for the first time enabled by this combination
    - The 3 coefficients are *strongly and differently* correlated in the individual channels → combining them breaks these degeneracies
    - VBF H→$\gamma\gamma$ not included due to its limited sensitivity in constraining the 3D parameter space
  - Both linear-only and linear + quadratic scenarios are considered
- Systematic uncertainties are correlated where applicable
  - Experimental uncertainties are fully correlated (luminosity, object reconstruction and calibration)
  - Theoretical uncertainties are correlated among analyses targeting the same H production mode
  - Background modelling uncertainties are uncorrelated
  - The impact of systematic uncertainties is small compared to the statistical error

Combined results: 1D fit on $c_{H\widetilde{W}}$

HIGP-2024-26

Linear-only

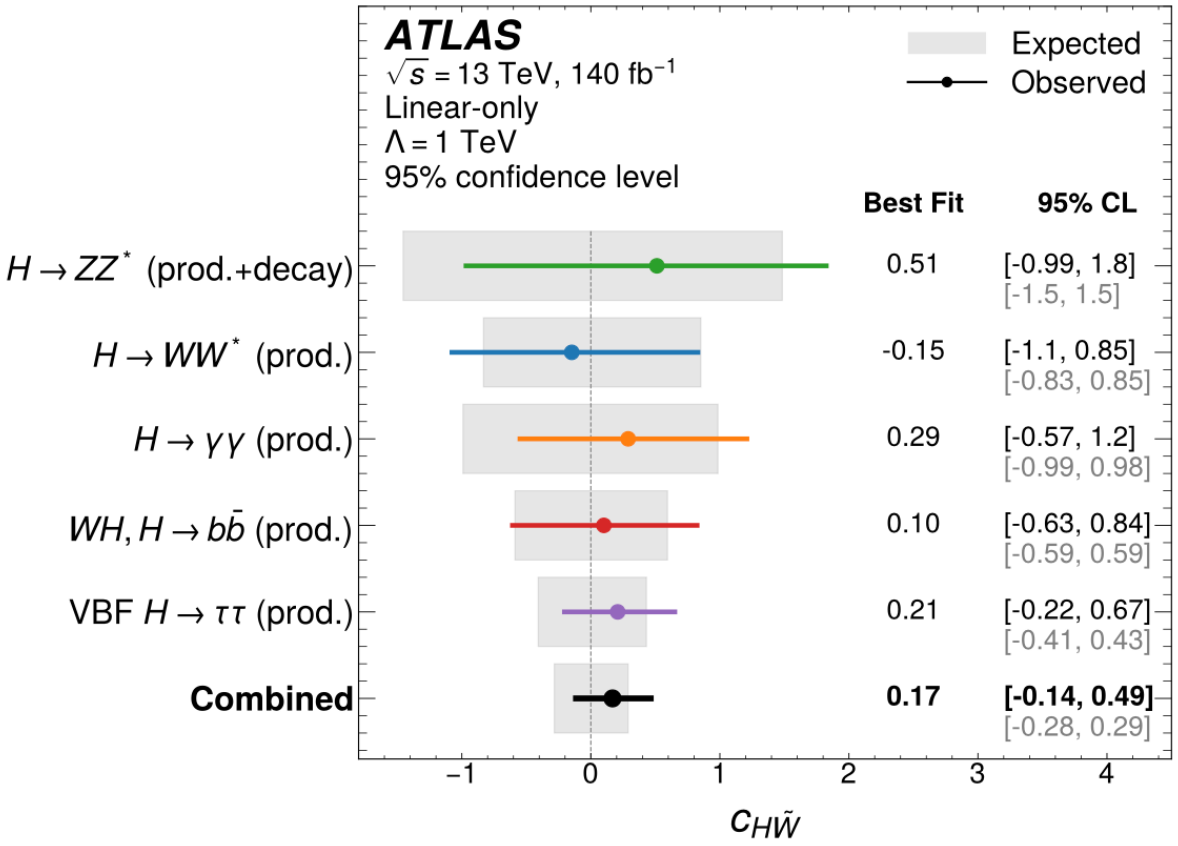

Linear + quadratic

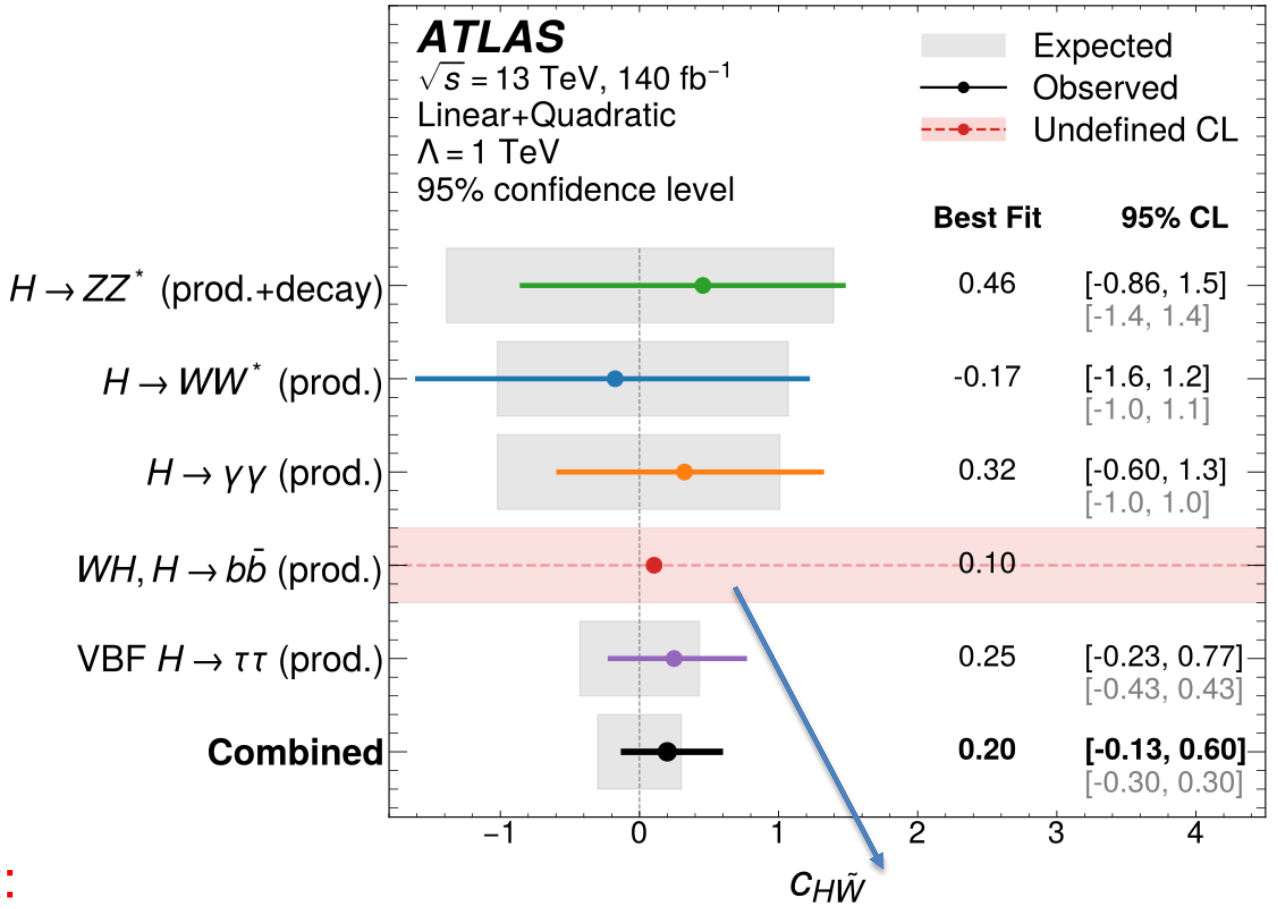

Combination brings significant improvement:

- ×3 better than H→ZZ*, H→WW* and H→$\gamma\gamma$
- ×2 better than WH H→bb
- 40% better than H→$\tau\tau$

For WH H→bb, the best-fit value is valid in the $c_{H\widetilde{W}}$ range [–1.5,1.5] and no 95%CL interval is defined

Combined results: 3D fit

HIGP-2024-26

3D ($c_{H\widetilde{W}}, c_{H\widetilde{B}}, c_{H\widetilde{W}B}$) fit results for the first time! Enabled by the combination

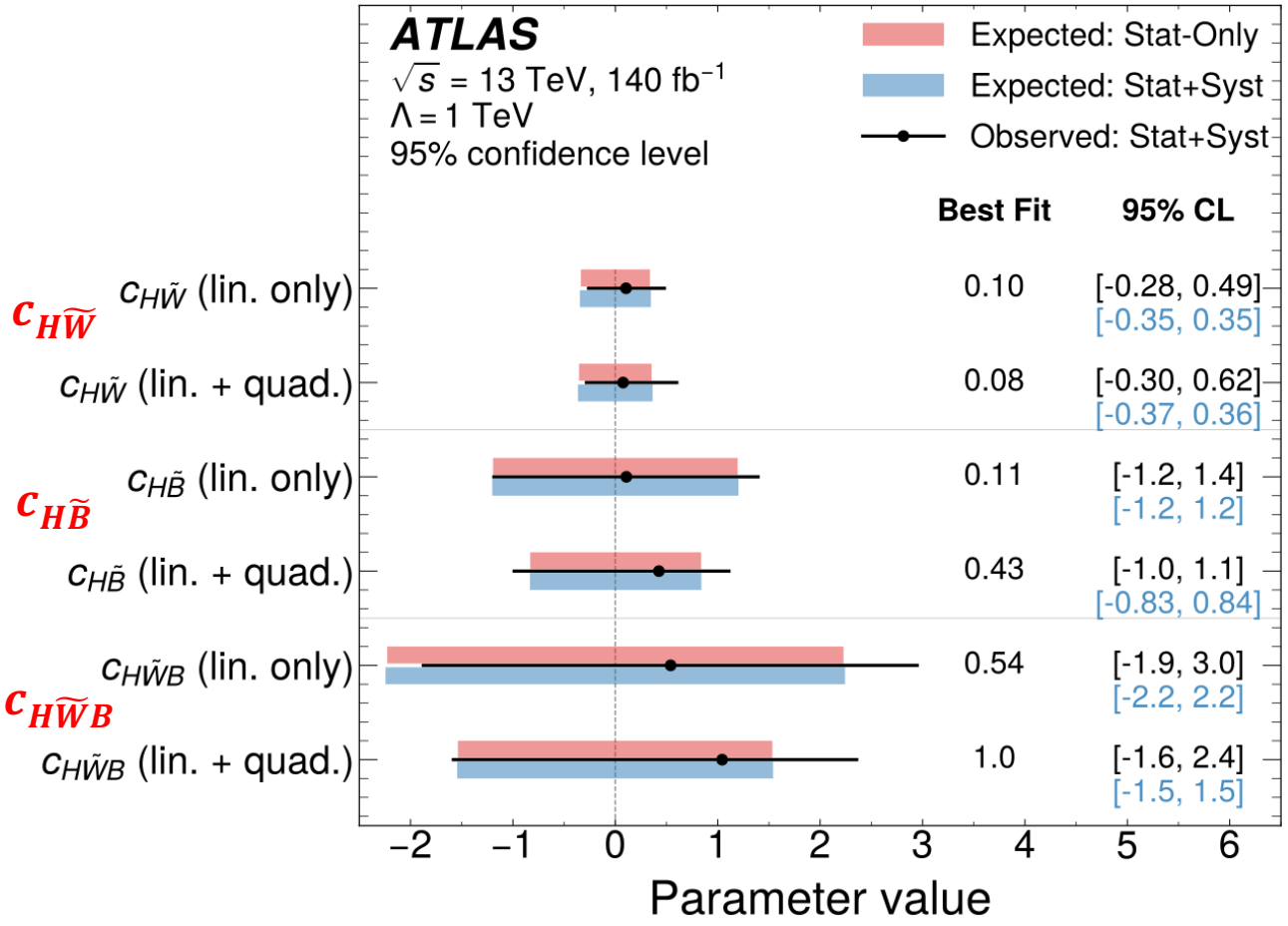

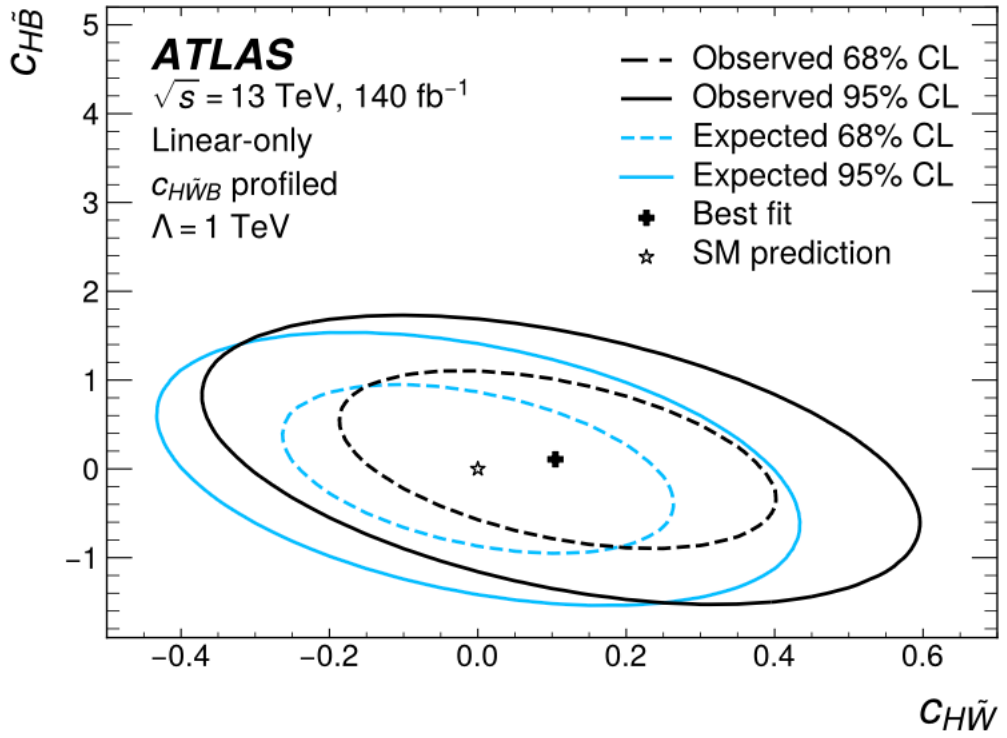

More 2D contours in the paper

Run3 VBF H$\gamma\gamma$ CP and Polarization

HIGP-2024-23

Analysis overview

- Probe BSM effects via precision measurements of the HVV tensor structure couplings
  - New sources of CP violation in the EFT framework
  - Polarization-dependent coupling
- VBF Higgs production with H→$\gamma\gamma$ decay, using 164 fb^{-1} of Run3 data
  - Select events with two isolated photons and two VBF tagging jets
  - A 3-class DNN used to discriminate VBF events from ggF and non-resonant background → refined classification algorithm w.r.t the Run2 analysis

$$D_{NN} = \log\left(\frac{p_{\mathrm{VBF}}}{\left(f_{\mathrm{ggH}} \cdot p_{ggF} + \left(1 - f_{\mathrm{ggH}}\right) \cdot p_{\mathrm{Continuum}}\right)}\right)$$

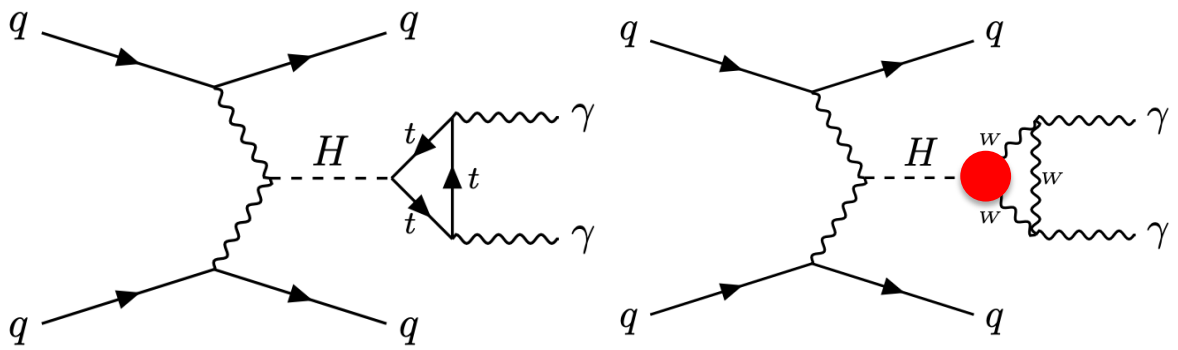

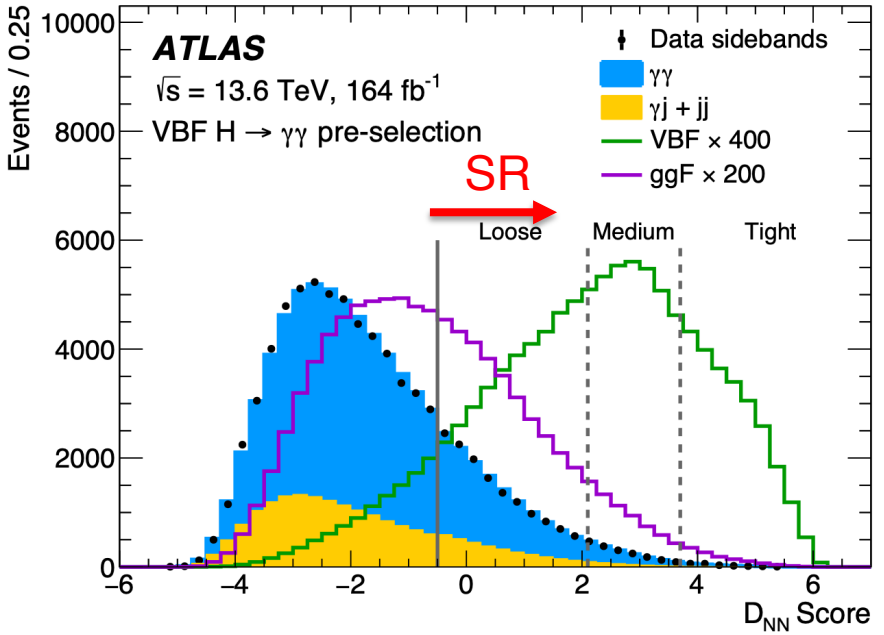

CP and Polarization observables

HIGP-2024-23

- CP
  - SMEFT Warsaw basis, focusing on $c_{H\widetilde{W}}$
  - Sensitive observable: OO defined as matrix element ratios

$$OO = \frac{2\mathrm{Re}(\mathcal{M}^{*}_{\mathrm{SM}}\mathcal{M}_{\mathrm{BSM}})}{|\mathcal{M}_{\mathrm{SM}}|^{2}}$$

- Polarization
  - Parametrize the polarization-dependent couplings

$$a_{\mathrm{L}} = \frac{g_{HV_{\mathrm{L}}V_{\mathrm{L}}}}{g_{HVV}} \qquad a_{\mathrm{T}} = \frac{g_{HV_{\mathrm{T}}V_{\mathrm{T}}}}{g_{HVV}}$$

  - In the SM: $a_L = a_T = 1$, while anomalous couplings predicted by BSM models, e.g., composite Higgs
  - Sensitive observable: the azimuthal angular difference between the two VBF-tagged jets, $\Delta\Phi_{jj}$
  - First time in H$\gamma\gamma$, previously only done in HWW*

EPJC 82 (2022) 622

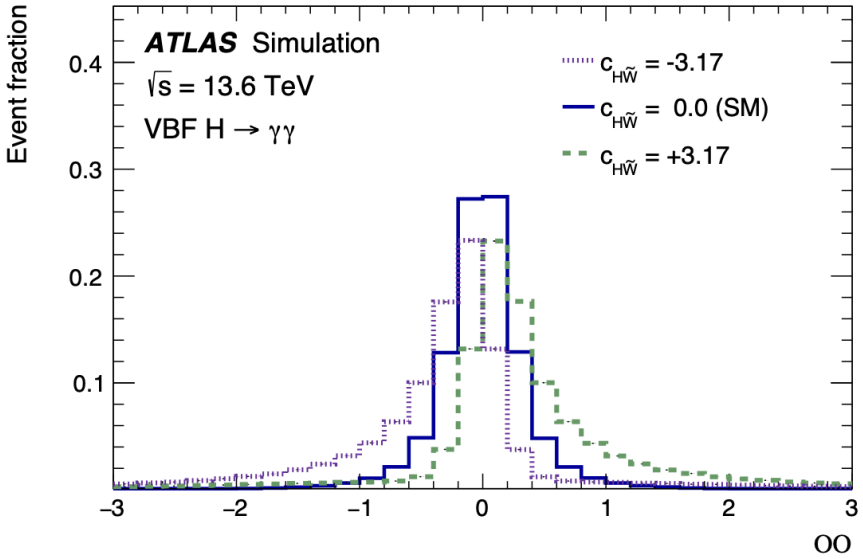

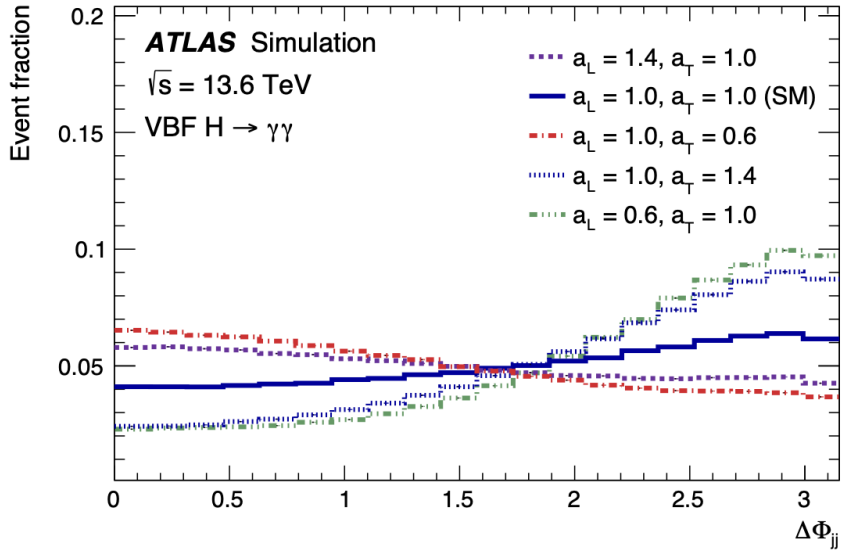

Results: Polarization measurements

HIGP-2024-23

Post-fit weighted $\Delta\Phi_{jj}$ distributions

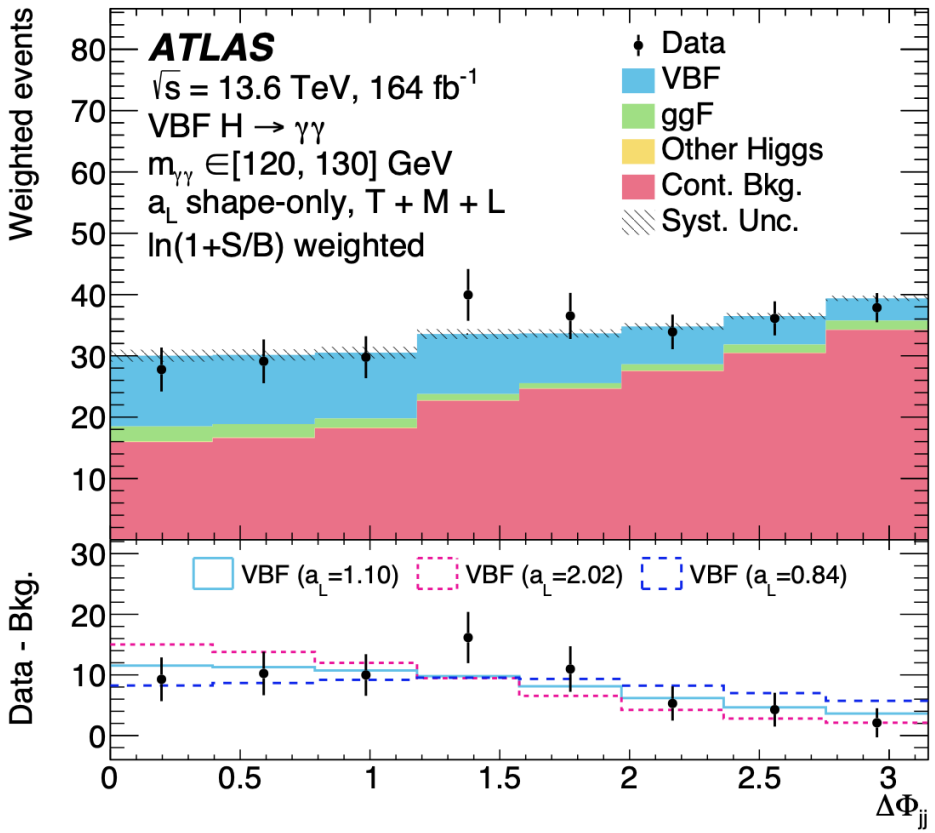

First ATLAS results to rely exclusively on fast detector simulation (AtlFast3)

Two distinct fits are considered: Shape-only and Shape + rate

a_L more strongly constrained by **rate** information

a_T more strongly constrained by the **shape** of the $\Delta\Phi_{jj}$

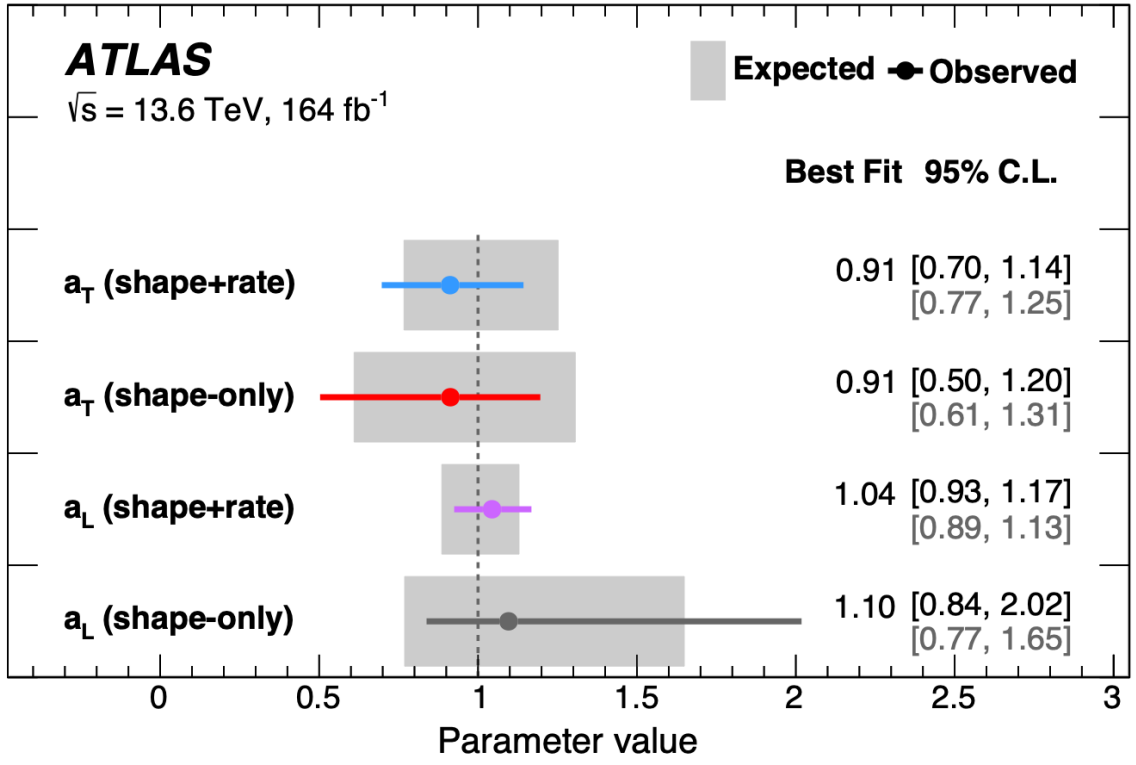

Significant improvement compared to the 36 fb^{-1} VBF HWW* (EPJC 82 (2022) 622): $\times 3$ better for shape + rate fit

Results: CP measurements

HIGP-2024-23

Both linear-only and linear + quadratic scenarios are considered

- Contribution of the quadratic terms found negligible

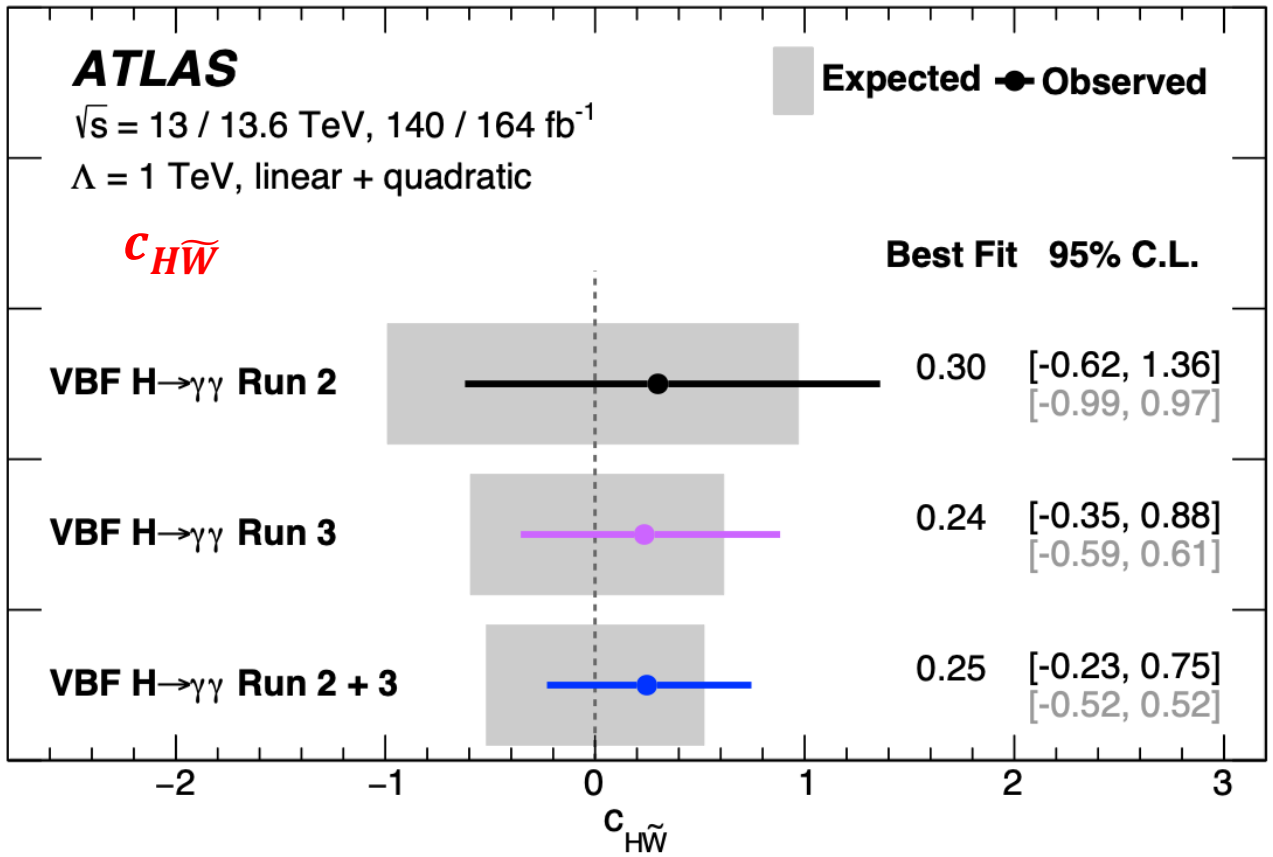

Run2 + Run3 combination to further improve the sensitivity

Constraints on $c_{H\widetilde{W}}$ are improved by ~50% → thanks to the new DNN classification algorithm

Still less stringent than the Run2 combination

(1D): $c_{H\widetilde{W}}$ linear + quadratic

Obs: [-0.13, 0.60]

Exp: [-0.30, 0.30]@ 95% CL

Run3 H4l STXS and differential measurements

ATLAS-CONF-2026-003

Analysis overview

- H→ZZ*→4l: golden channel for precision measurements
- Updated fiducial, differential and STXS measurements with 164 fb^{-1} of Run3 data
  - First inclusive prod. cross-section measurement at 13.6 TeV with 29 fb^{-1} data: EPJC 84 (2024) 78
  - Differential measurements with 2022-23 data, 56 fb^{-1}: ATLAS-CONF-2025-002

EPJC 84 (2024) 78

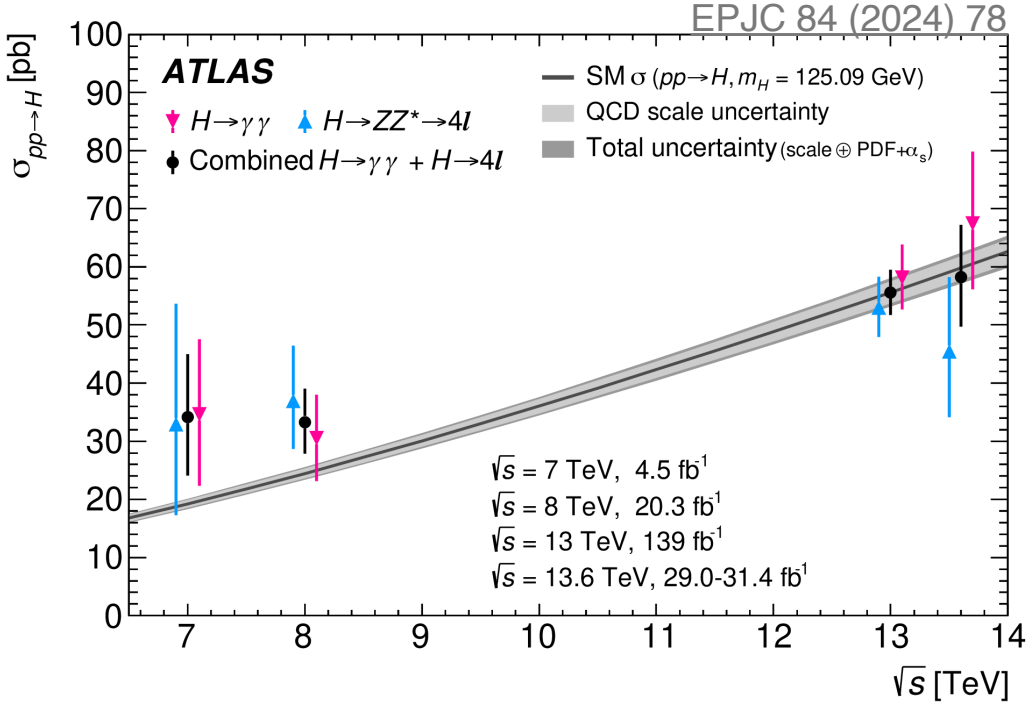

ATLAS-CONF-2025-002

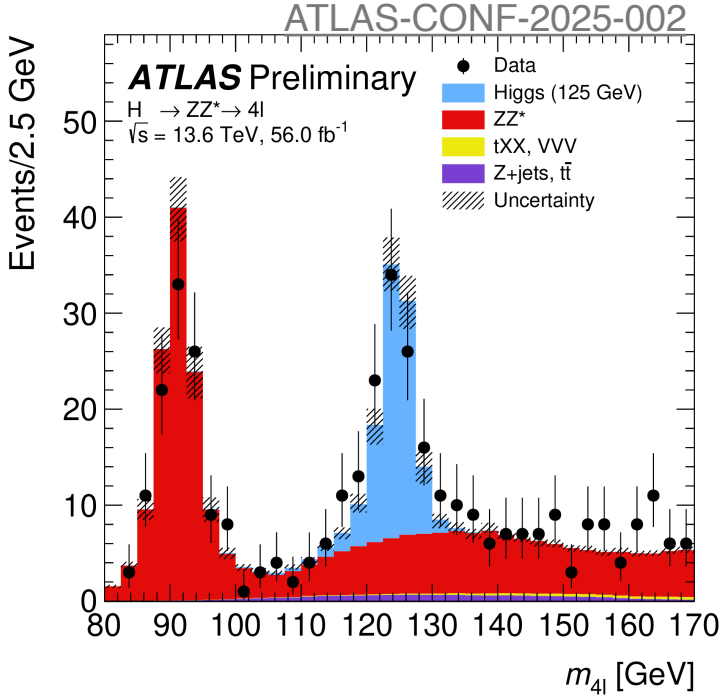

Analysis overview

ATLAS-CONF-2026-003

- H→ZZ*→4l: golden channel for precision measurements
- Updated fiducial, differential and STXS measurements with 164 fb^{-1} of Run3 data

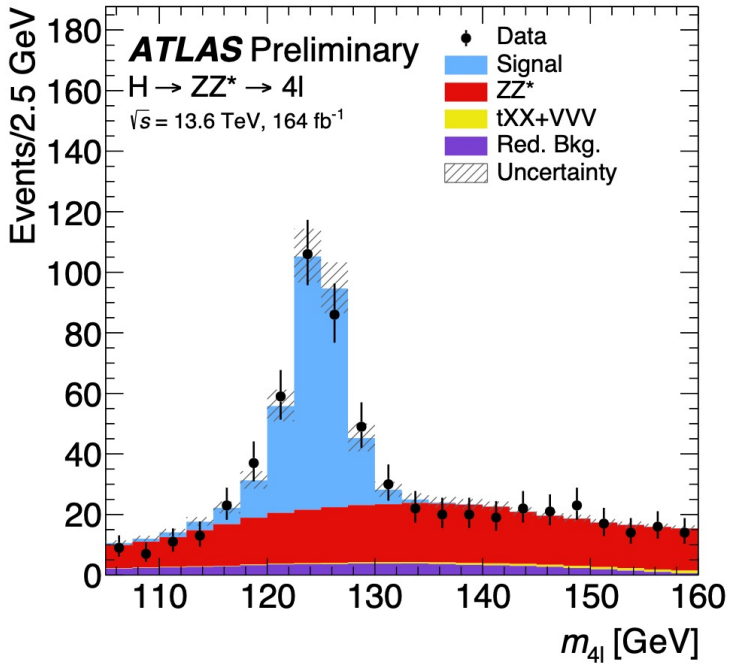

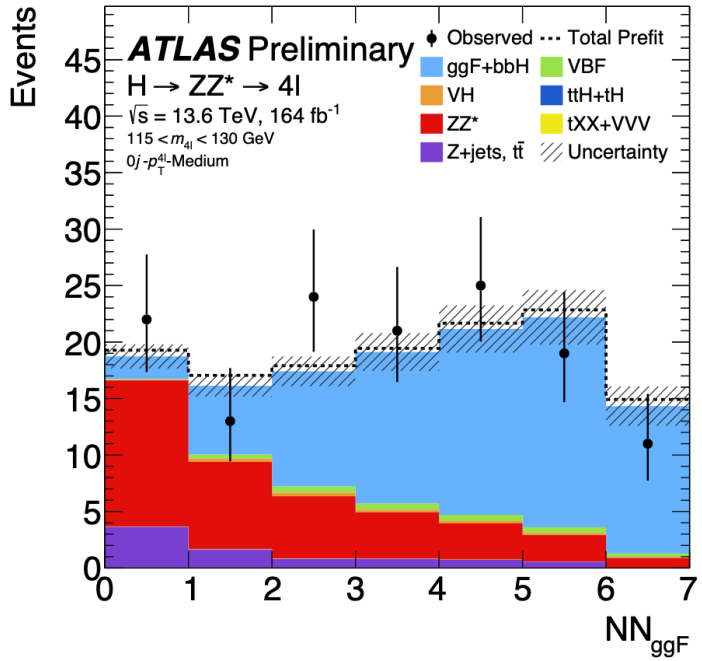

Backgrounds:

- Non-resonant ZZ* normalization from m4l sideband
- Non-prompt bkg (Z+jets, ttbar) from a data-driven fake factor method

Fiducial and differential measurements:

- Cross-sections extracted from binned likelihood fit using m_{4l} spectrum
- Detector effects are corrected through an likelihood-based matrix unfolding procedure

STXS:

- Discriminants based on a Set Transformer architecture
- Results extracted from simultaneous fit of signal regions and sidebands to constrain the ZZ* and tXX normalizations

Inclusive fiducial and total cross-sections

ATLAS-CONF-2026-003

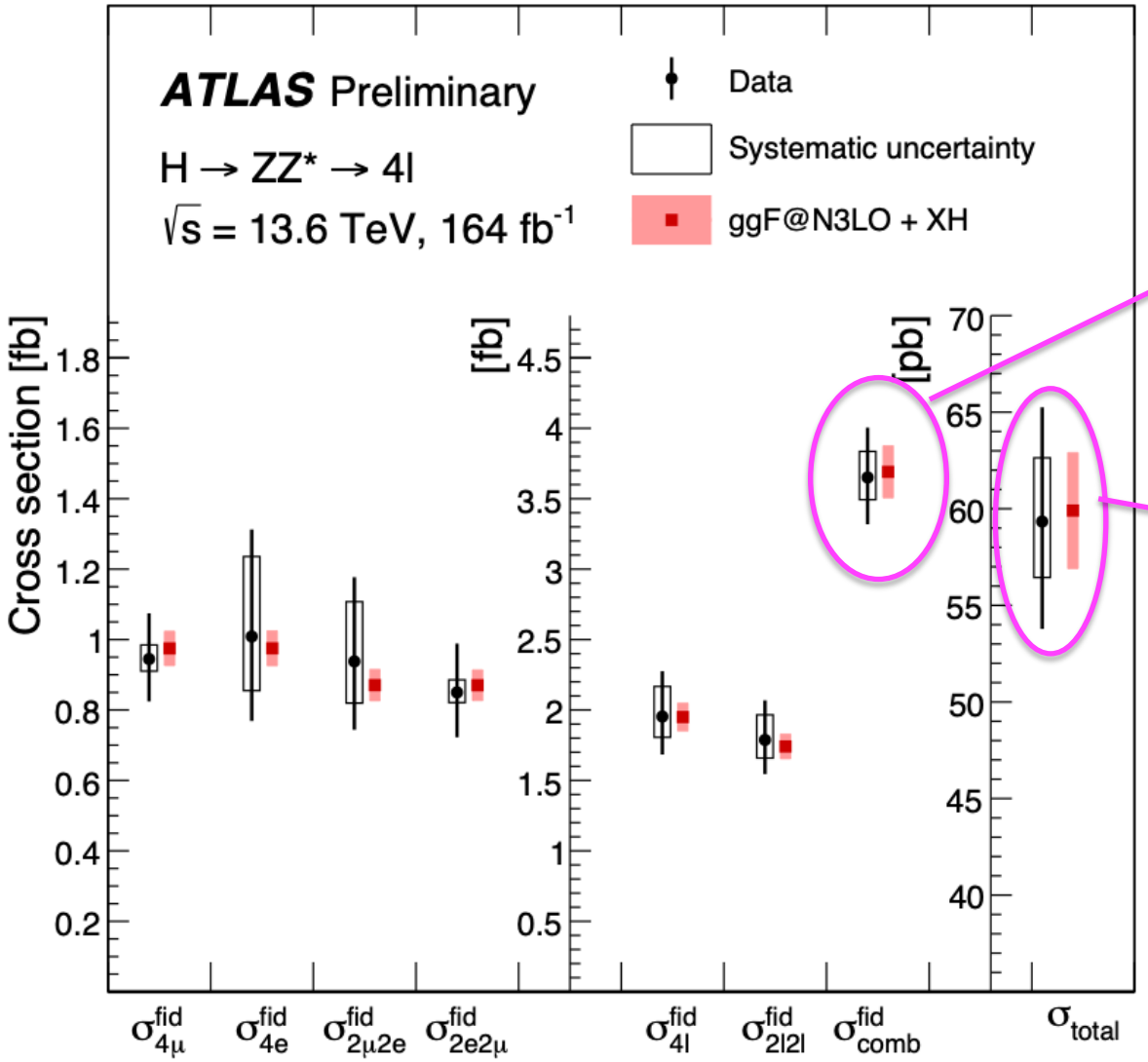

Fiducial cross-section

$$\sigma_{fid} = \sigma \cdot \mathrm{B}(H \to ZZ^* \to 4l)$$
$$= 3.65 \pm 0.30(\mathrm{stat.})\,^{+0.18}_{-0.16}(\mathrm{sys.})\mathrm{fb} = \mathbf{3.65}^{+0.35}_{-0.33}\ \mathbf{fb}$$

$$\sigma^{\mathrm{SM}}_{\mathrm{fid}} = 3.68 \pm 0.17\ \mathrm{pb}$$

Total cross-section

$$\sigma_{\mathrm{total}} = 59.3 \pm 4.8(\mathrm{stat.}) \pm 3.1(\mathrm{sys.})\mathrm{pb}$$
$$= \mathbf{59.3} \pm \mathbf{5.7\ pb}$$

$$\sigma^{\mathrm{SM}}_{\mathrm{total}} = 59.9 \pm 3.0\ \mathrm{pb}$$

Good agreement with the state-of-the-art SM predictions

Differential cross-sections

ATLAS-CONF-2026-003

Good agreement with the state-of-the-art SM predictions

More differential measurements at the backup

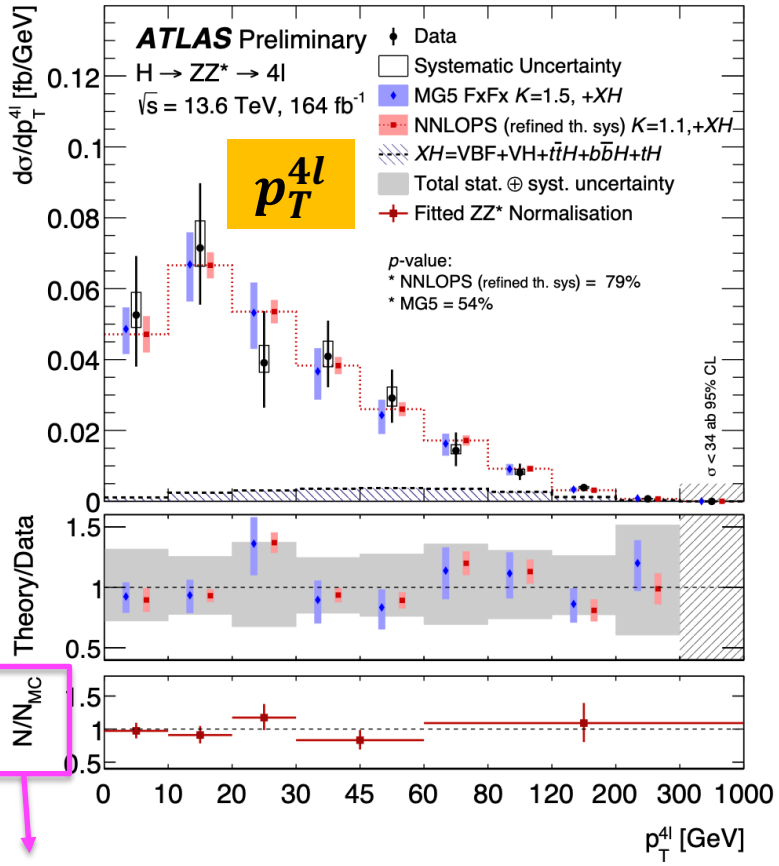

ZZ* normalization factors

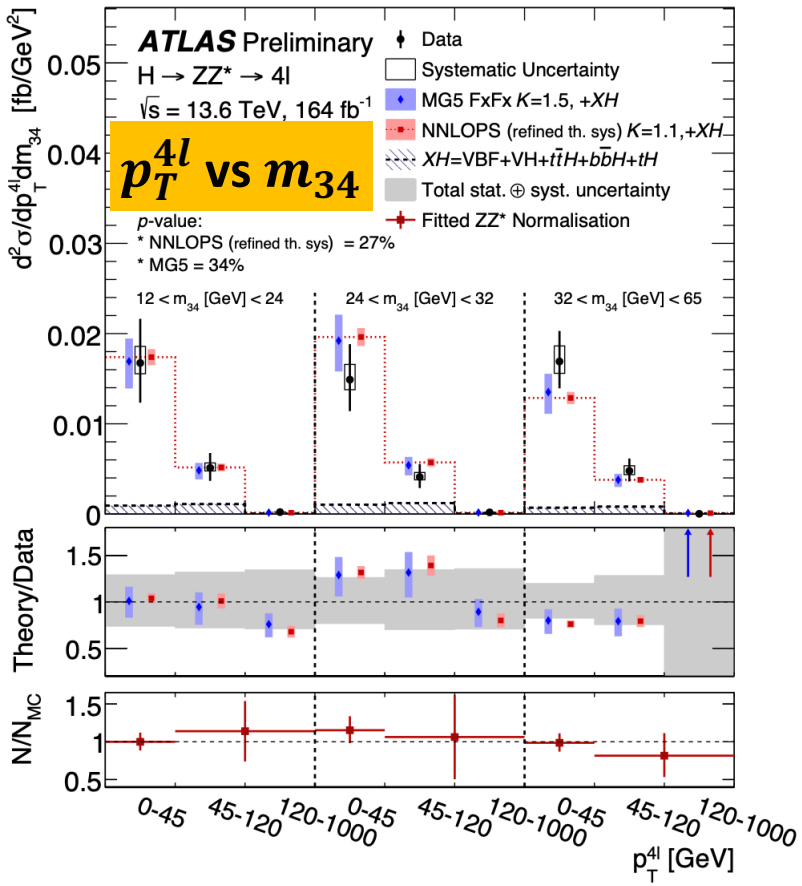

Sensitive to BSM effects

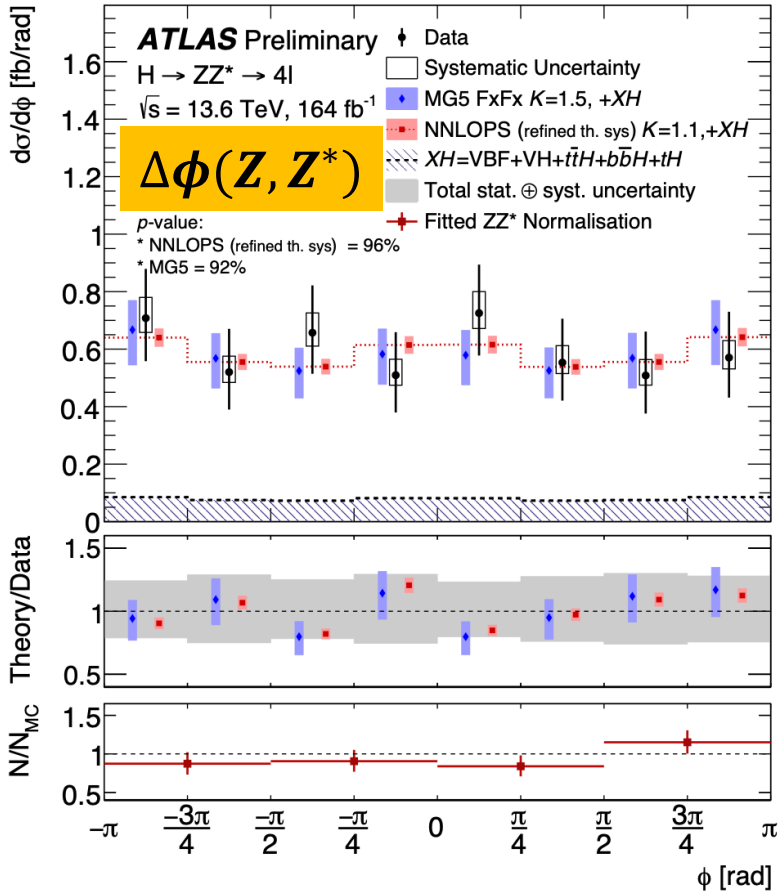

Recover sensitivity to SM-BSM interference effects

STXS results

ATLAS-CONF-2026-003

Good agreement with the state-of-the-art SM predictions

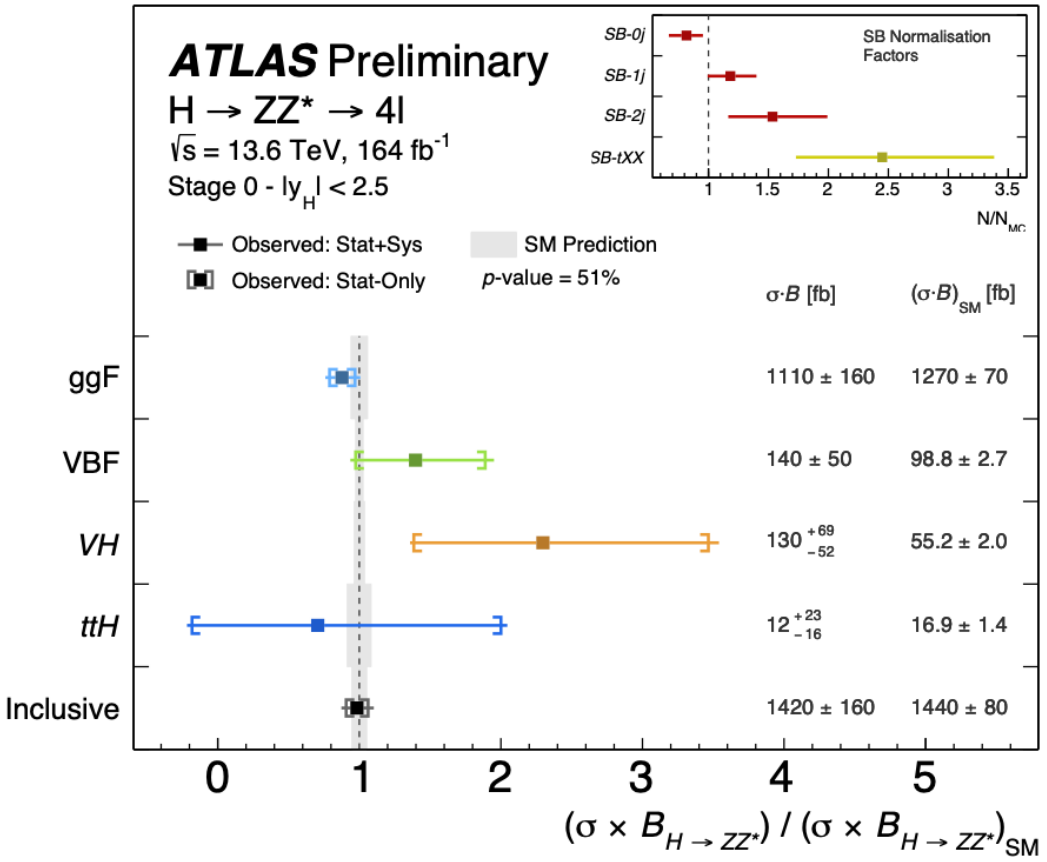

Production mode (stage 0)

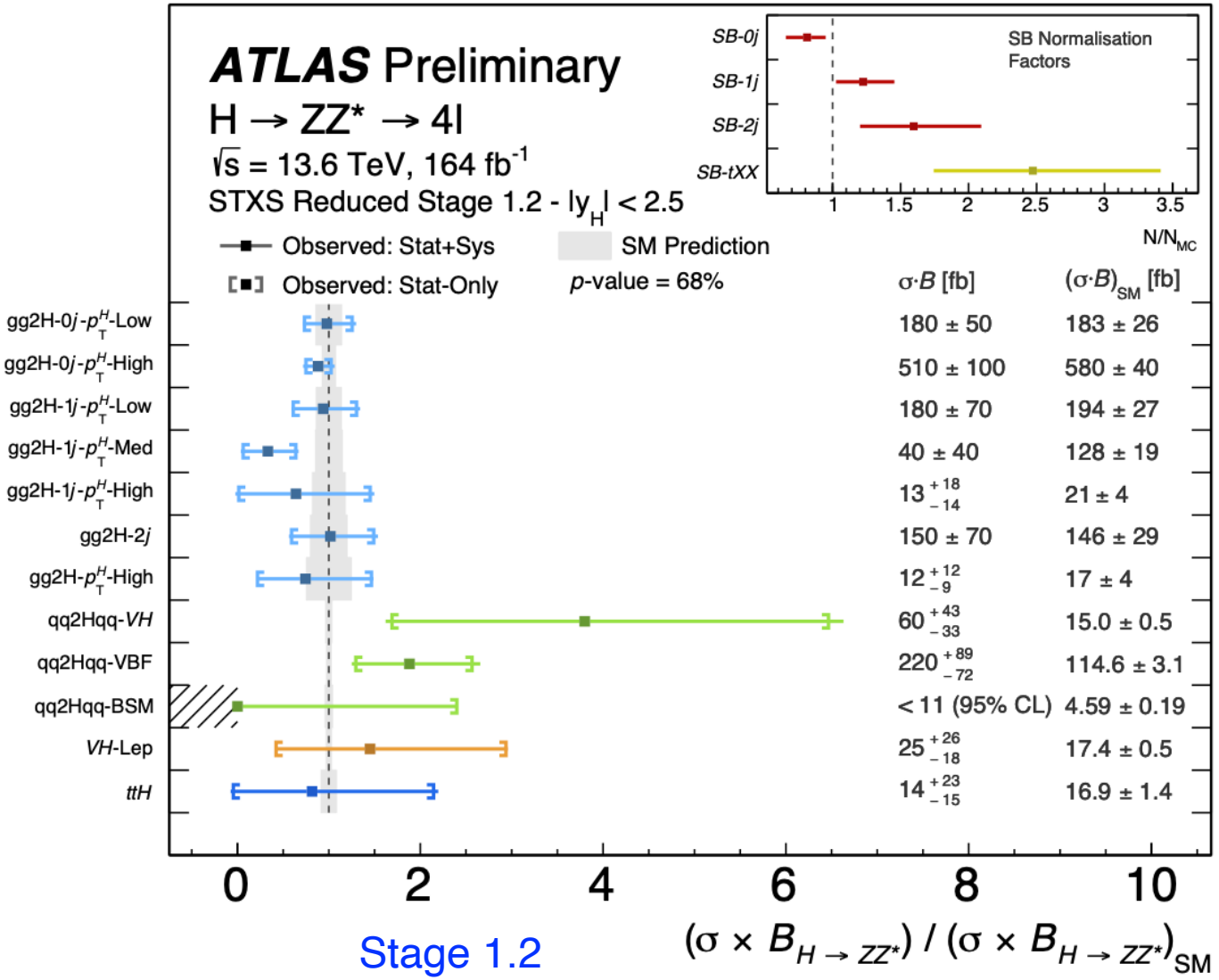

Stage 1.2

Interpretations: κ-framework ATLAS-CONF-2026-003

Measured production mode (Stage 0) cross-sections are interpreted in the κ-framework with (κ_V, κ_f)

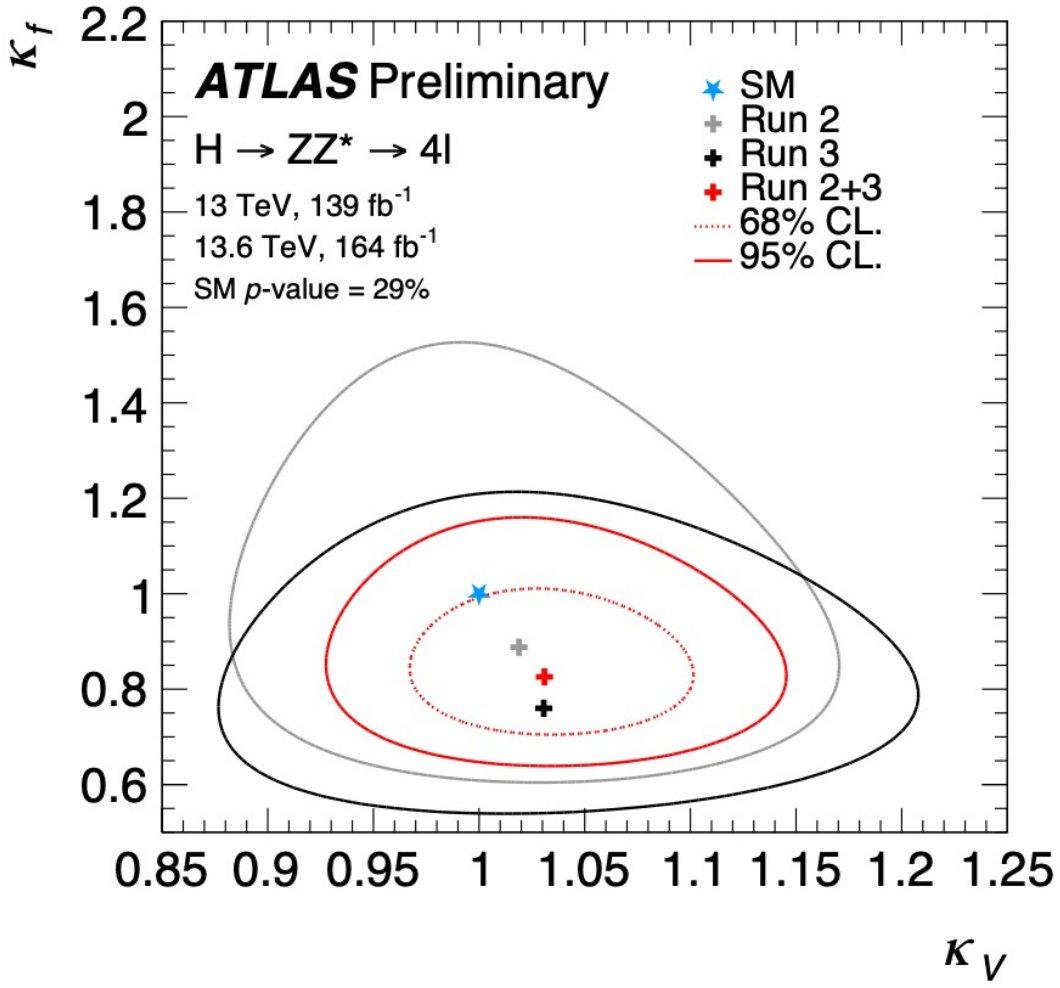

Coupling-strength modifier $\kappa \equiv \frac{\lambda}{\lambda_{SM}}$

A benchmark scenario with two universal modifiers:

$$\kappa_V = \kappa_W = \kappa_Z$$
$$\kappa_f = \kappa_t = \kappa_b = \kappa_c = \kappa_\tau = \kappa_\mu$$

Also performed statistical combination of Run2+Run3 to further improve the sensitivity:
~40%(25%) better for κ_V (κ_f) compared to Run2 results

Interpretations: SMEFT

ATLAS-CONF-2026-003

Interpretations of differential measurements

- CP-even scans performed using m_{34}, $\mathrm{p_T^{4l}}$ vs m_{34}, and Φ
- CP-odd scans performed using Φ and $\Delta\Phi_{jj}$
- Observables with the best expected sensitivity used for limits (Φ, except $\mathrm{p_T^{4l}}$ vs m_{34} used for $\boldsymbol{c_{HW}}$)

		Expected 95% CL [TeV^{-2}]		Observed 95% CL [TeV^{-2}]		Best fit [TeV^{-2}]	
		Linear	Linear + Quadratic	Linear	Linear + Quadratic	Linear	Linear + Quadratic
CP-even	c_{HW}	$[-3.8, 3.2]$	$[-1.8, 1.8]$	$[-4.3, 2.9]$	$[-2.0, 1.8]$	-0.40	-0.08
	c_{HB}	$[-0.63, 0.59]$	$[-0.54, 1.2]$	$[-0.58, 0.64]$	$[-0.49, 1.25]$	0.05	0.05
	c_{HWB}	$[-1.5, 1.4]$	$[-0.42, 0.48]$	$[-1.6, 1.3]$	$[-0.40, 0.45]$	-0.08	-0.02
CP-odd	$c_{H\tilde{W}}$	$[-3.0, 3.0]$	$[-1.6, 1.6]$	$[-2.1, 3.9]$	$[-1.3, 1.6]$	0.88	0.38
	$c_{H\tilde{B}}$	$[-1.5, 1.5]$	$[-1.0, 0.96]$	$[-1.1, 1.6]$	$[-0.80, 0.96]$	0.39	0.20
	$c_{H\tilde{W}B}$	$[-2.3, 2.3]$	$[-0.45, 0.45]$	$[-3.1, 1.5]$	$[-0.44, 0.41]$	-0.80	-0.09

Limits on Wilson coefficients (1D fit)

2D fits also performed

Interpretations: the trilinear Higgs self-coupling

- λ_3 enters single-H production/decay at one-loop through electroweak corrections
- Can therefore be constrained using precision measurements of single-H observables
  - p_T^{4l} differential measurements
  - STXS measurements

$$\kappa_\lambda = \frac{\lambda_3}{\lambda_3^{SM}}$$

$$\Sigma_{\lambda_3}^{\mathrm{BSM}}(\kappa_\lambda) = Z_H^{BSM}\,\Sigma_{LO}(1 + \kappa_\lambda C_1(\{p_n\}) + \delta Z_H)$$

$$Z_H^{\mathrm{BSM}} = \frac{1}{1 - (\kappa_\lambda^2 - 1)\,\delta Z_H}$$

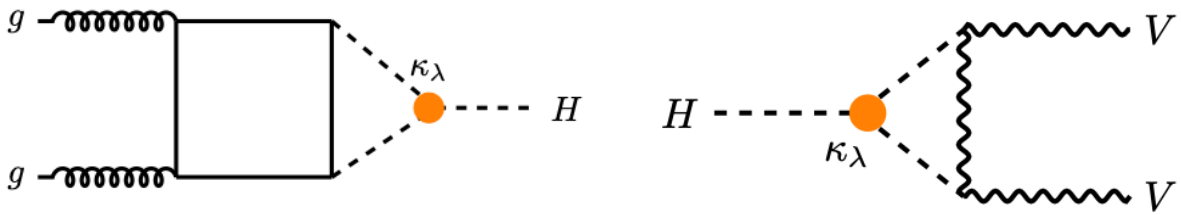

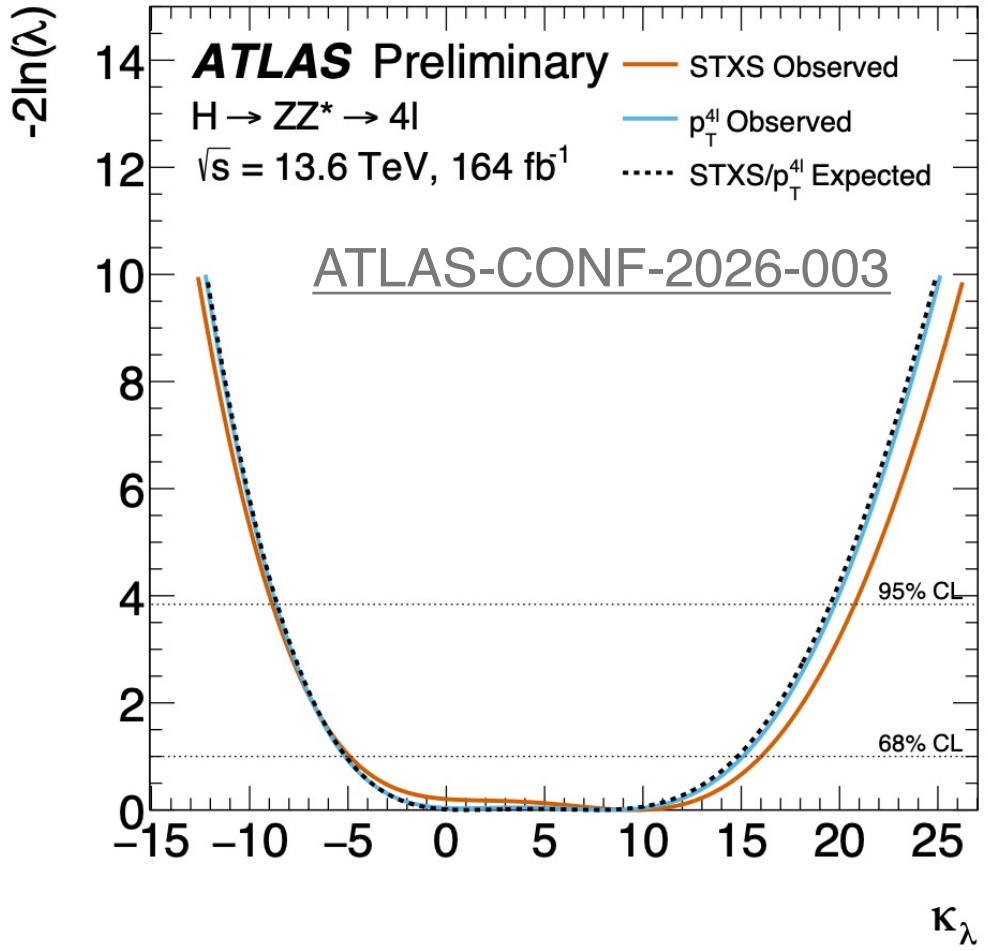

Summary

- Presented *hot-off-the-press* single-Higgs measurements from ATLAS
- Run2 HVV CP combination: HIGP-2024-26
  - Deliver the most stringent constraints on CP-violating Wilson coefficients in the SMEFT framework
  - The first multi-channel CP-violation measurement in the HVV interaction by the ATLAS experiment
- Run3 VBF H$\gamma\gamma$ CP and Polarization measurements HIGP-2024-23
  - Updated constraints on CP-odd parameter $c_{H\widetilde{W}}$ (by 50% compared to Run2)
  - First polarization-dependent couplings a_L, a_T in this channel
- Updated Run3 H4l STXS and differential measurements ATLAS-CONF-2026-003
  - Improved precision with lumi 56 fb^{-1} → 164 fb^{-1} and refined analysis methods
  - Comprehensive interpretations: $\boldsymbol{\kappa}$-framework, SMEFT, κ_λ self-coupling

- All measurements consistent with the SM but with significantly improved precisions
- More results are coming and looking forward for full Run3 (~ 300 fb^{-1})!

Backup

Run2 HVV CP combination: 3D fit

HIGP-2024-26

3D $(c_{H\widetilde{W}}, c_{H\widetilde{B}}, c_{H\widetilde{W}B})$ fit results for the first time!

Linear-only

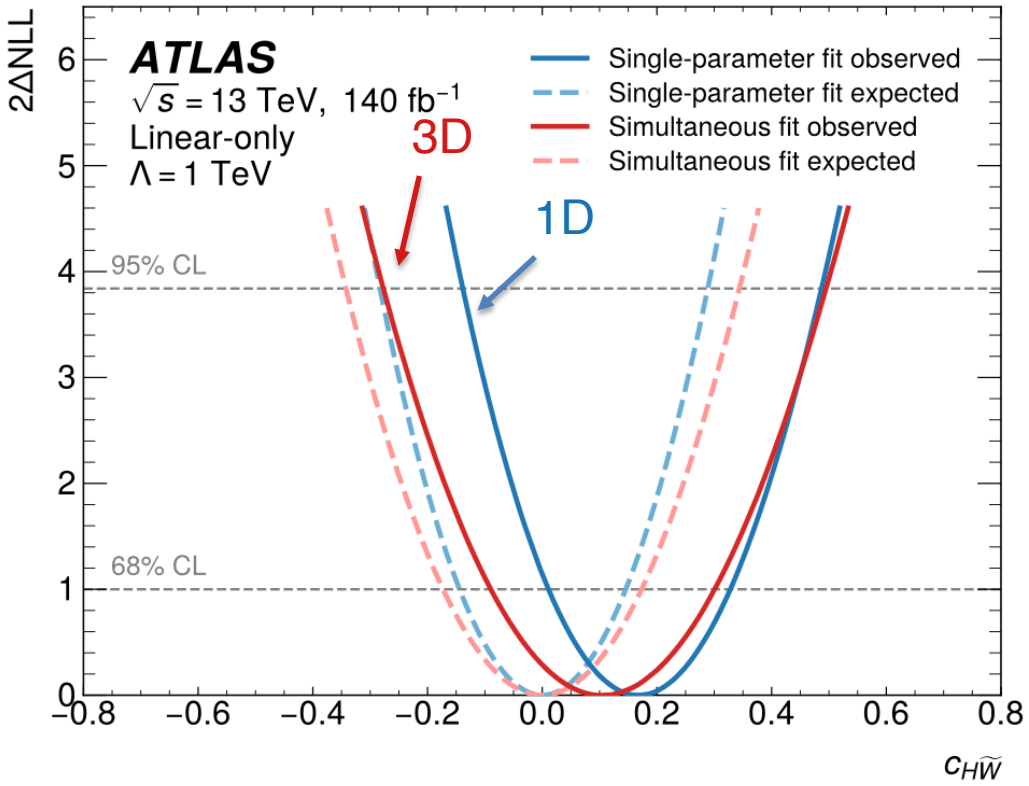

Linear + quadratic

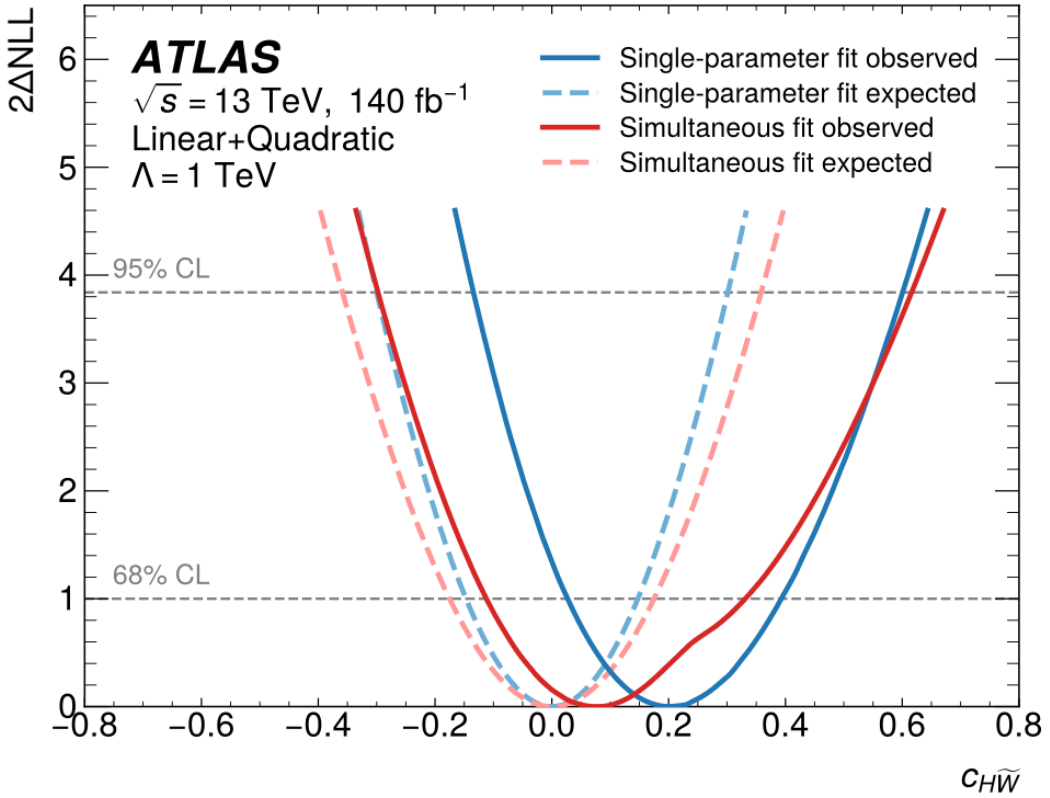

The limits obtained in the 3D fit are less stringent than those obtained in the 1D fit, due to the negative correlation between $c_{H\widetilde{W}}$ and $c_{H\widetilde{B}}, c_{H\widetilde{W}B}$

Run2 HVV CP combination

HIGP-2024-26

linear-only, expected

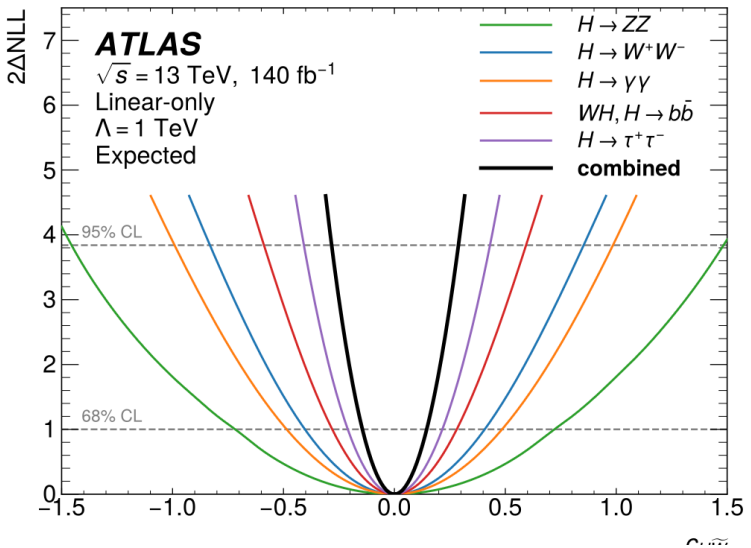

linear-only, observed

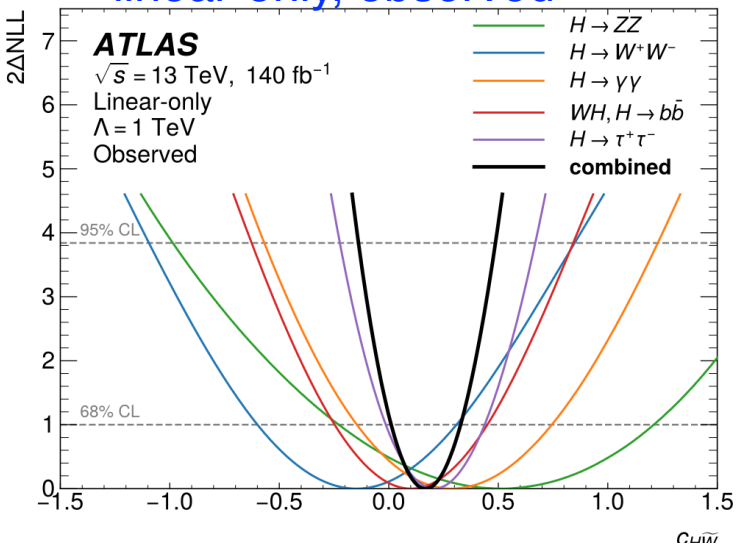

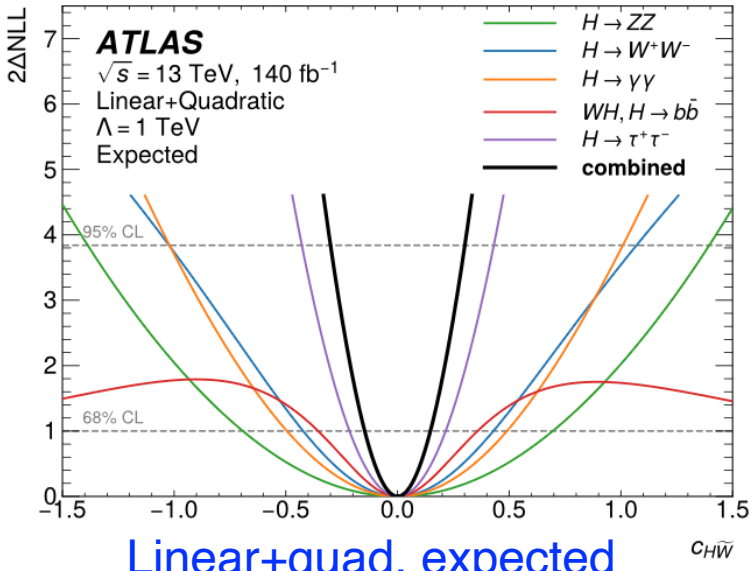

Linear+quad, expected

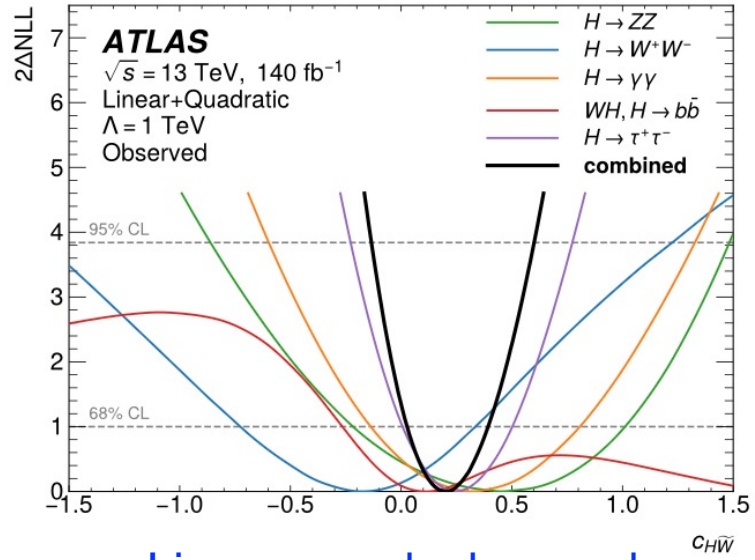

Linear+quad, observed

The non-trivial shape of WHbb:

- Linear-only: the asymmetry grows linearly with $c_{H\widetilde{W}}$
- Linear+quad: the asymmetry grows approximately linearly only for small values of $c_{H\widetilde{W}}$ and is then much reduced (or even inverted)

$$\mu_p \rightarrow \mu_p \times (1 + \sum_{j=1}^{M} A_j^p \times c_j + B_j^p \times c_j^2),$$

$$\mathrm{Asym}_{p,j}^{\mathrm{linear}} = -A_j^p \times c_j$$

$$\mathrm{Asym}_{p,j}^{\mathrm{linear+quadratic}} = \frac{-A_j^p \times c_j}{1 + B_j^p \times c_j^2}$$

Run2 HVV CP combination

HIGP-2024-26

Limits on the new physics scale Λ (1D fit)

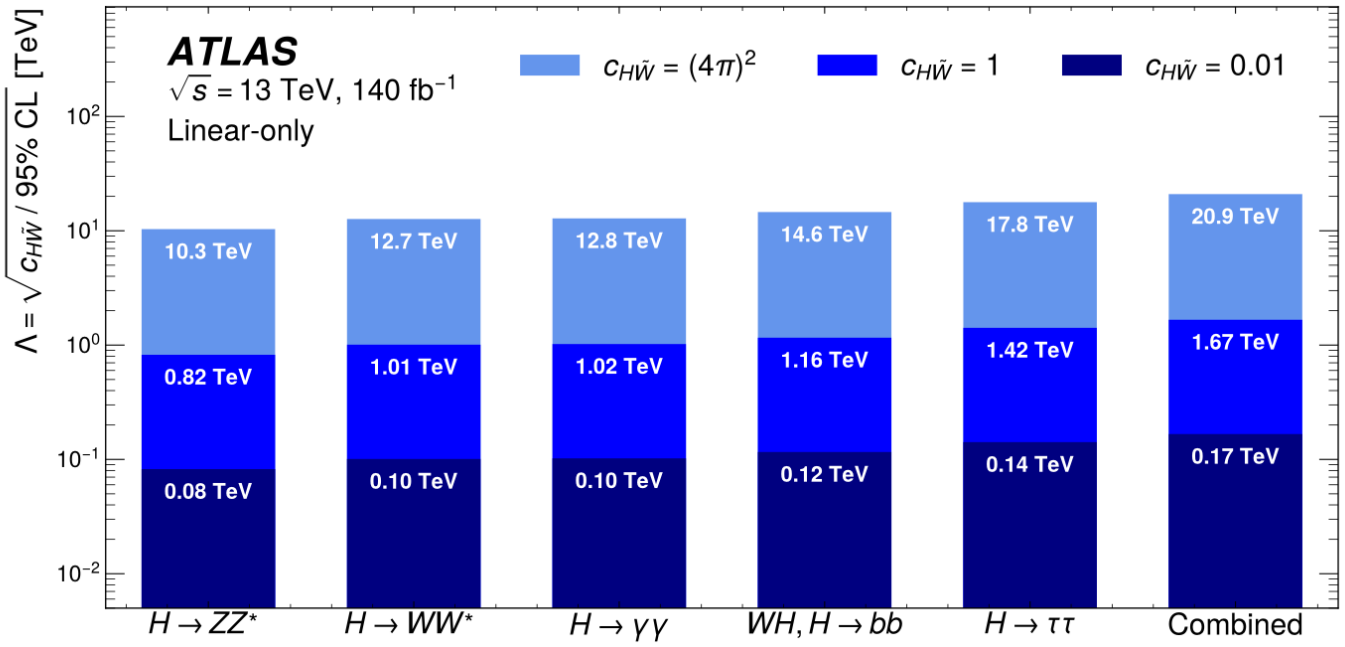

Limits on the new physics scale Λ (3D fit)

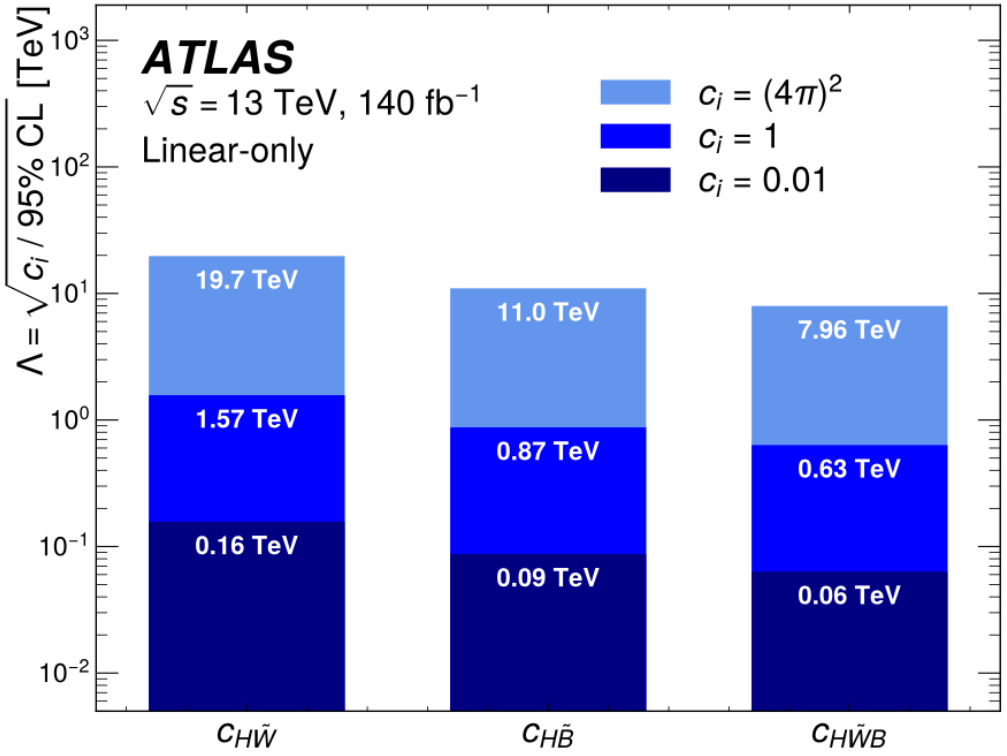

Run3 VBF H$\gamma\gamma$ CP and Polarization

HIGP-2024-23

Event-level selection requirements		
Preselection	Number of selected photons	$N_\gamma \geq 2$
	Number of selected jets	$N_j \geq 2$
Suppression of continuum background	Invariant di-photon mass	$105\,\text{GeV} < m_{\gamma\gamma} \leq 160\,\text{GeV}$
	Transverse momentum of the leading photon relative to the invariant di-photon mass	$p_{\text{T},\gamma_1}/m_{\gamma\gamma} > 0.35$
	Transverse momentum of the subleading photon relative to the invariant di-photon mass	$p_{\text{T},\gamma_2}/m_{\gamma\gamma} > 0.25$
VBF topology	Pseudorapidity gap between the two leading jets	$\Delta\eta_{jj} > 2.0$
	Zeppenfeld observable	$\lvert\eta^{\text{Zepp}}\rvert < 5.0$
	DNN response score requirement	$D_{NN} > -0.5$

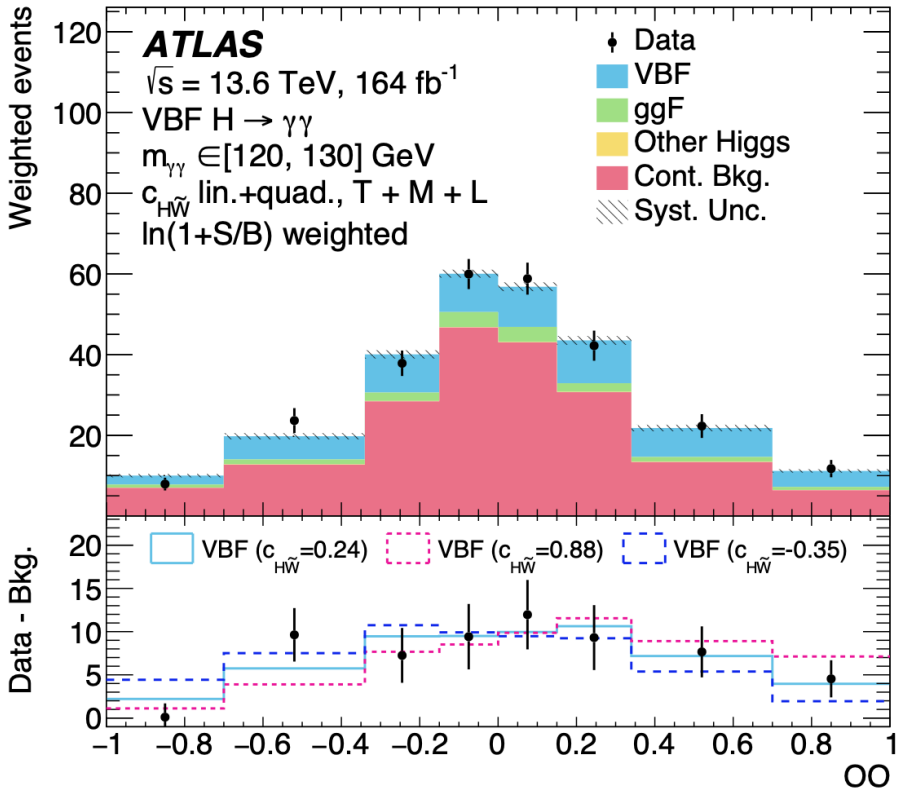

Run3 VBF H$\gamma\gamma$ CP and Polarization

HIGP-2024-23

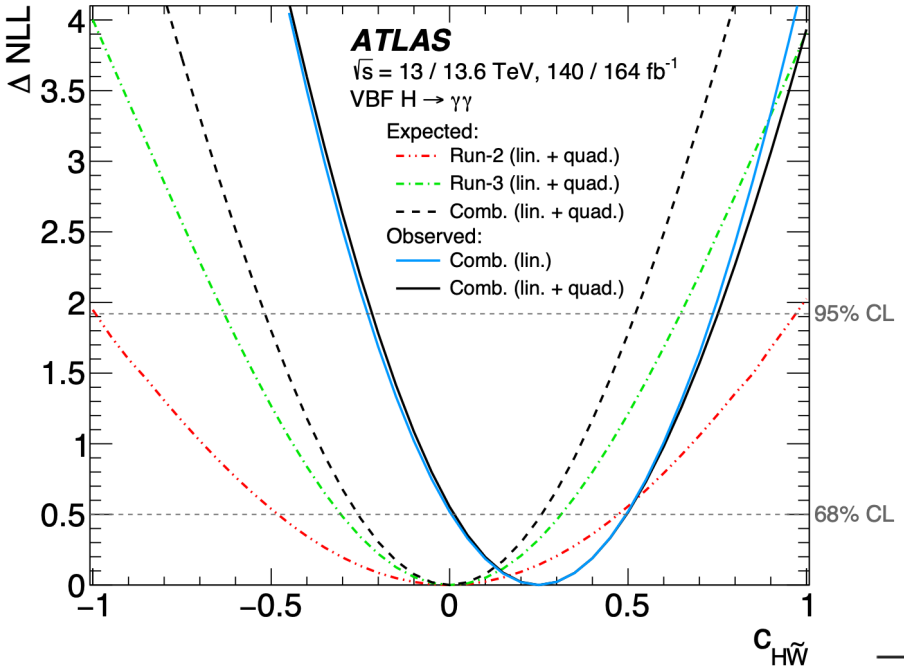

negligible impact of the quadratic terms

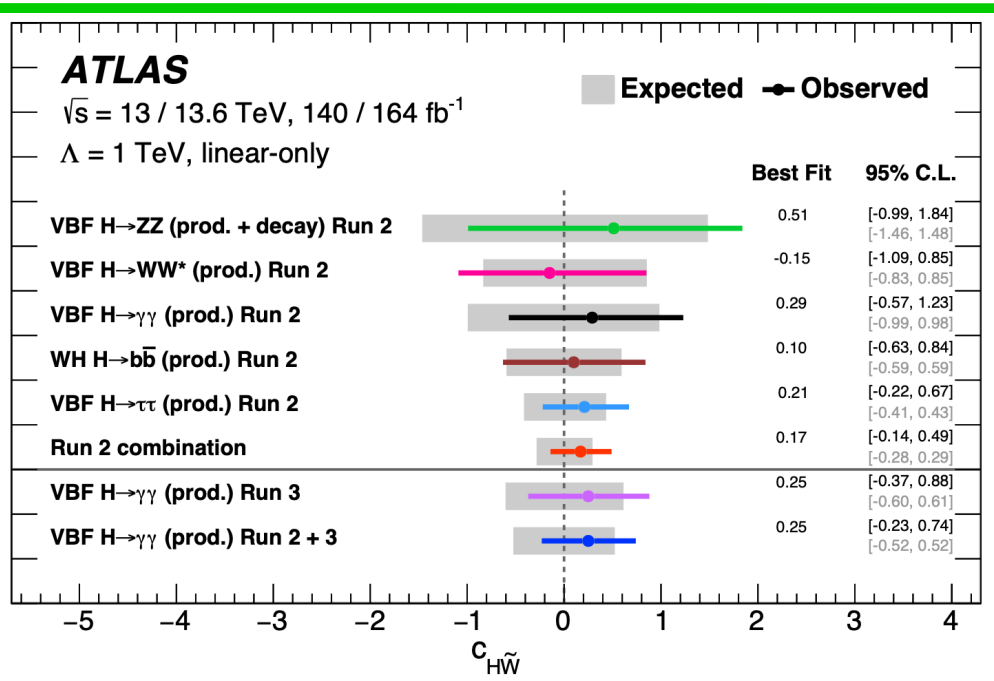

Source	$c_{H\widetilde{W}}$ (Linear-only)	$c_{H\widetilde{W}}$ (Linear+quad.)	a_{L} (shape-only)	a_{L} (shape+rate)	a_{T} (shape-only)	a_{T} (shape+rate)
Total statistical	99%	99%	98%	79%	98%	89%
Total systematic	10%	7.4%	20%	61%	20%	45%
Spurious Signal	12%	11%	9.1%	7.4%	9.3%	7.4%
G4-AF3 discrepancies	3.3%	4.8%	2.1%	18%	3.3%	12%
Photons	< 1%	< 1%	2.9%	22%	3.9%	16%
Jets	7.0%	9.3%	10%	38%	12%	24%
Luminosity + Pile-up	1.6%	1.9%	< 1%	9.4%	< 1%	7.0%
VBF theory	5.8%	5.4%	8.8%	31%	9.5%	23%
ggF theory	2.9%	4.0%	5.0%	5.1%	6.1%	5.9%
Other Higgs boson theory	< 1%	< 1%	< 1%	< 1%	< 1%	< 1%

Run3 VBF H$\gamma\gamma$ CP and Polarization HIGP-2024-23

	Expected results		Observed results		
	68% CL	95% CL	Best-fit value	68% CL	95% CL
$c_{H\widetilde{W}}$ (linear-only)	[-0.303, 0.311]	[-0.603, 0.610]	0.247	[-0.067, 0.564]	[-0.374, 0.881]
$c_{H\widetilde{W}}$ (linear+quadratic)	[-0.286, 0.300]	[-0.594, 0.614]	0.235	[-0.058, 0.544]	[-0.354, 0.883]
a_{L} (shape-only)	[0.872, 1.213]	[0.769, 1.649]	1.096	[0.944, 1.361]	[0.838, 2.018]
a_{L} (shape+rate)	[0.946, 1.068]	[0.886, 1.129]	1.044	[0.984, 1.105]	[0.925, 1.168]
a_{T} (shape-only)	[0.824, 1.148]	[0.610, 1.306]	0.913	[0.737, 1.060]	[0.503, 1.196]
a_{T} (shape+rate)	[0.874, 1.112]	[0.767, 1.252]	0.912	[0.803, 1.025]	[0.697, 1.143]

Run2 HWW* (36/fb), EPJC 82 (2022) 622

Type	Expected	Observed
a_{T} shape-only fit ($a_{\mathrm{L}} = 1$)	$1.0 \pm 0.5(\mathrm{stat.})^{+0.3}_{-0.4}(\mathrm{syst.})$	$1.3^{+0.8}_{-0.4}(\mathrm{stat.})^{+0.3}_{-0.2}(\mathrm{syst.})$
a_{L} shape + rate fit ($a_{\mathrm{T}} = 1$)	$1.00^{+0.08}_{-0.10}(\mathrm{stat.})^{+0.07}_{-0.13}(\mathrm{syst.})$	$0.90^{+0.09}_{-0.13}(\mathrm{stat.})^{+0.08}_{-0.18}(\mathrm{syst.})$
a_{T} shape + rate fit ($a_{\mathrm{L}} = 1$)	$1.00^{+0.36}_{-0.49}(\mathrm{stat.})^{+0.19}_{-0.27}(\mathrm{syst.})$	$1.19^{+0.27}_{-0.32}(\mathrm{stat.})^{+0.12}_{-0.14}(\mathrm{syst.})$
a_{L} shape + rate fit (a_{T} profiled)	$1.00^{+0.08}_{-0.10}(\mathrm{stat.})^{+0.08}_{-0.13}(\mathrm{syst.})$	$0.91^{+0.10}_{-0.18}(\mathrm{stat.})^{+0.09}_{-0.17}(\mathrm{syst.})$
a_{T} shape + rate fit (a_{L} profiled)	$1.0^{+0.4}_{-0.5}(\mathrm{stat.})^{+0.2}_{-0.4}(\mathrm{syst.})$	$1.2 \pm 0.4(\mathrm{stat.})^{+0.2}_{-0.3}(\mathrm{syst.})$

Run3 H4l

ATLAS-CONF-2026-003

Final state	Signal	ZZ^*	Other Backgrounds	Total SM	Observed
4μ	90.5 ± 5.3	41.2 ± 1.6	4.5 ± 0.3	136 ± 6	136
$2e2\mu$	63.4 ± 4.0	30.0 ± 1.3	4.7 ± 0.5	98 ± 5	98
$2\mu2e$	40.7 ± 9.1	15.6 ± 4.4	5.6 ± 0.2	62 ± 13	67
$4e$	36.5 ± 9.2	14.1 ± 4.3	5.3 ± 0.3	56 ± 13	59
Total	231 ± 23	101 ± 10	20.1 ± 1.3	352 ± 32	360

Input variables for STXS NN discriminants

Category	Process	Global inputs	Lepton set inputs	Jet set inputs	Discriminant
$0j$-$p_{\mathrm{T}}^{4\ell}$-Low $0j$-$p_{\mathrm{T}}^{4\ell}$-Med	ggF, ZZ^*	$\eta_{4\ell}$, $p_{\mathrm{T},4\ell}$, D_{ZZ^*}, m_{12} m_{34}, $\cos\theta^*$, $\cos\theta_1$, ϕ_{ZZ}	$p_{\mathrm{T},\ell}$, η_ℓ	–	$\mathrm{NN_{ggF}}$
$1j$-$p_{\mathrm{T}}^{4\ell}$-Low	ggF, VBF, ZZ^*	$p_{\mathrm{T},4\ell}$, $p_{\mathrm{T},j}$, η_j, D_{ZZ^*} $\Delta R_{4\ell,j}$,$\eta_{4\ell}$, $E_{\mathrm{T}}^{\mathrm{miss}}$	$p_{\mathrm{T},\ell}$, η_ℓ	–	$\mathrm{NN_{ggF+VBF}}$ for $\mathrm{NN_{ZZ}}$<0.2 $\mathrm{NN_{ZZ}}$ for $\mathrm{NN_{ZZ}}$>0.2
$1j$-$p_{\mathrm{T}}^{4\ell}$-Med	ggF, VBF, ZZ^*	$p_{\mathrm{T},4\ell}$, $p_{\mathrm{T},j}$, η_j, D_{ZZ^*} $\Delta R_{4\ell,j}$,$\eta_{4\ell}$, $E_{\mathrm{T}}^{\mathrm{miss}}$	$p_{\mathrm{T},\ell}$, η_ℓ	–	$\mathrm{NN_{ggF+VBF}}$ for $\mathrm{NN_{ZZ}}$<0.2 $\mathrm{NN_{ZZ}}$ for $\mathrm{NN_{ZZ}}$>0.2
$1j$-$p_{\mathrm{T}}^{4\ell}$-High	ggF, VBF	$p_{\mathrm{T},4\ell}$, $p_{\mathrm{T},j}$, η_j, D_{ZZ^*} $\Delta R_{4\ell,j}$,$\eta_{4\ell}$, $E_{\mathrm{T}}^{\mathrm{miss}}$	$p_{\mathrm{T},\ell}$, η_ℓ	–	$\mathrm{NN_{ggF}}$
$2j$	ggF, VBF, VH	m_{jj}, $p_{\mathrm{T},4\ell jj}$, $\eta_{ZZ}^{\mathrm{zepp}}$	$p_{\mathrm{T},\ell}$, η_ℓ	$p_{\mathrm{T},j}$, η_j, m_j	$\mathrm{NN_{ggF}}$ for $\mathrm{NN_{VH}}$<0.3, $\mathrm{NN_{VBF}}$<0.1 $\mathrm{NN_{VBF}}$ for $\mathrm{NN_{VH}}$<0.3, $\mathrm{NN_{VBF}}$>0.1 $\mathrm{NN_{VH}}$ for $\mathrm{NN_{VH}}$>0.3, $\mathrm{NN_{VBF}}$<0.1
$2j$-BSM-like	ggF, VBF	m_{jj}, $p_{\mathrm{T},4\ell jj}$, $\eta_{ZZ}^{\mathrm{zepp}}$	$p_{\mathrm{T},\ell}$, η_ℓ	$p_{\mathrm{T},j}$, η_j, m_j	$\mathrm{NN_{VBF}}$

Run3 H4l

ATLAS-CONF-2026-003

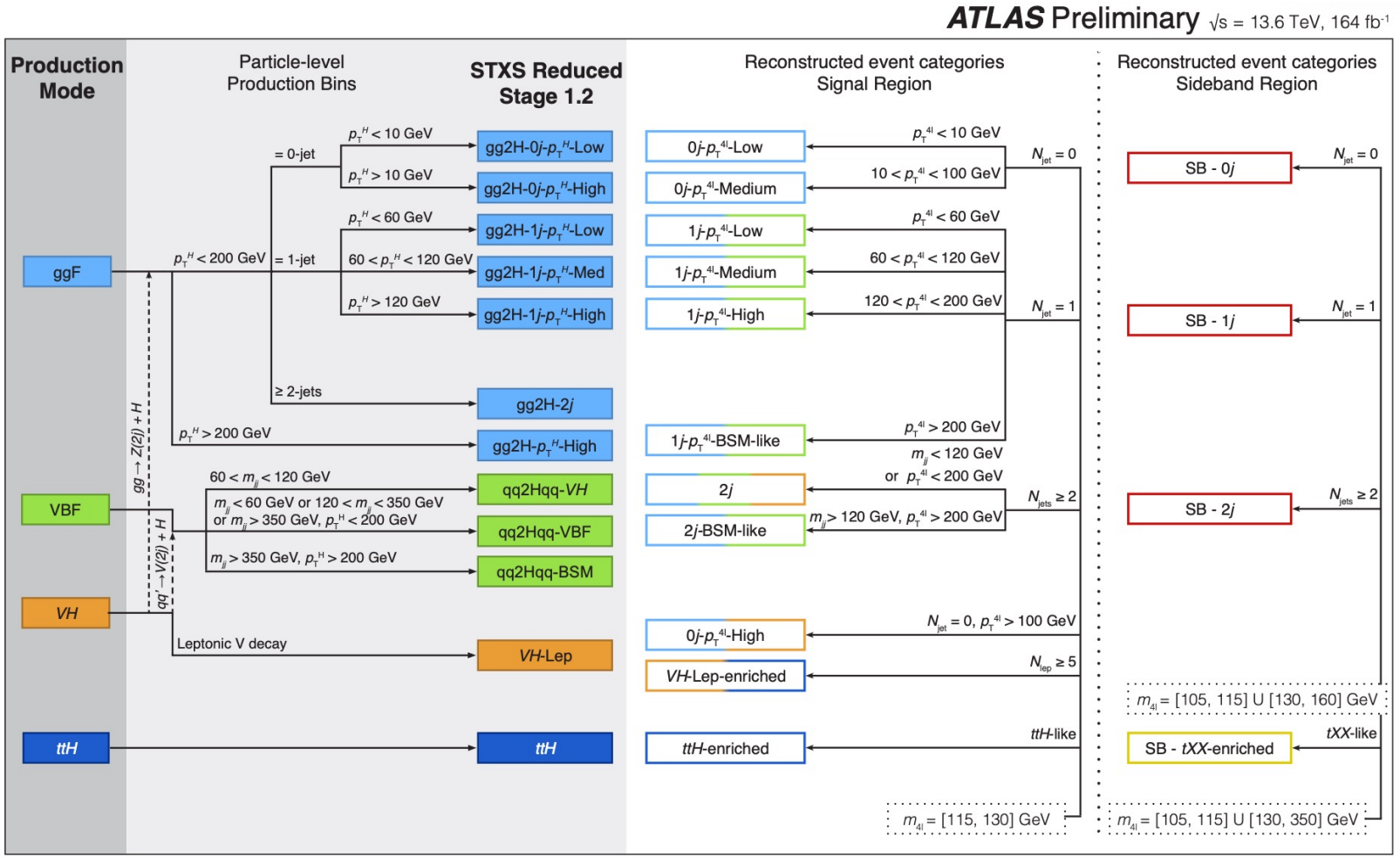

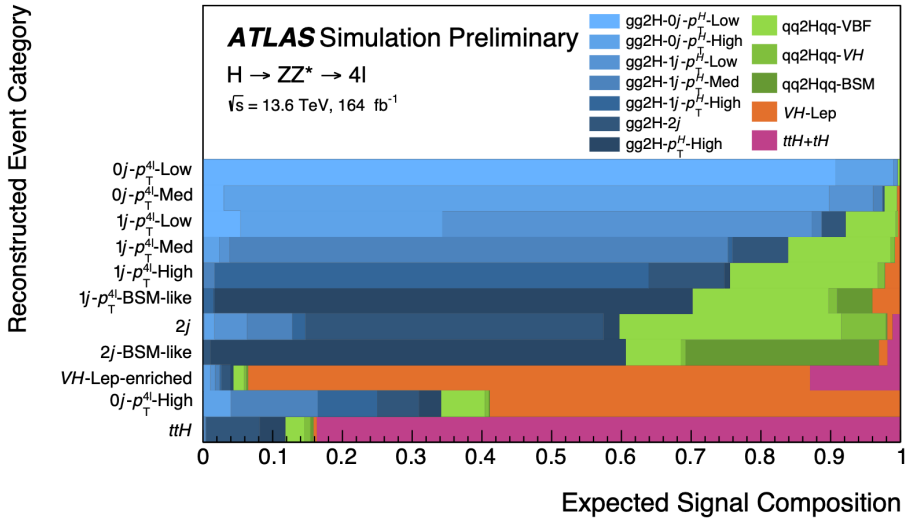

Run3 H4l

ATLAS-CONF-2026-003

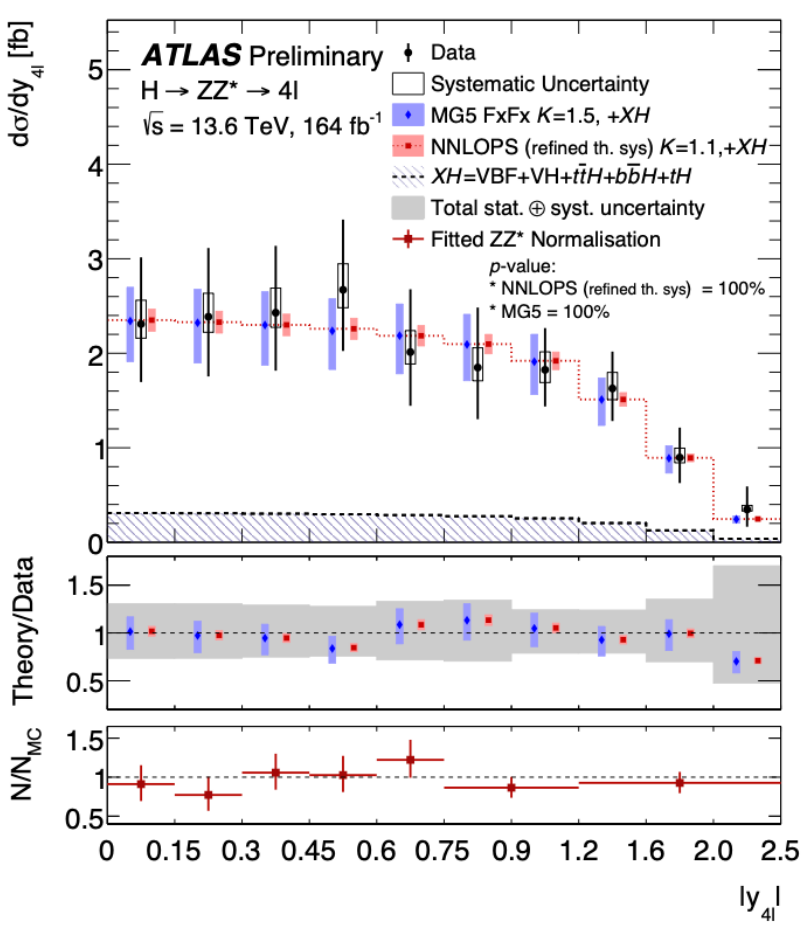

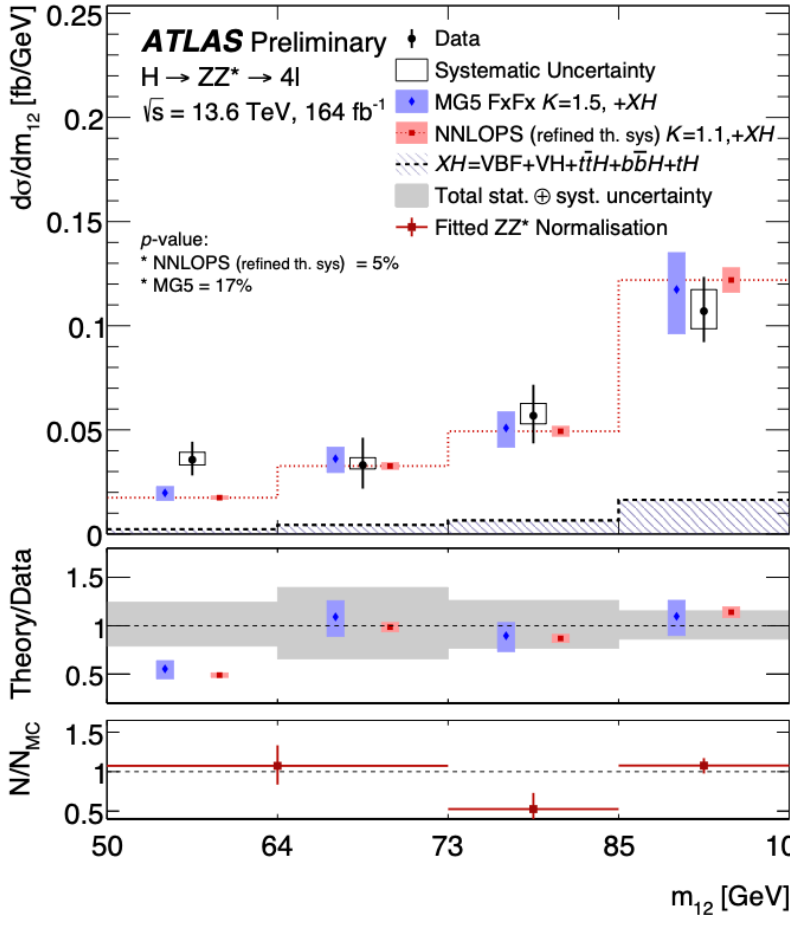

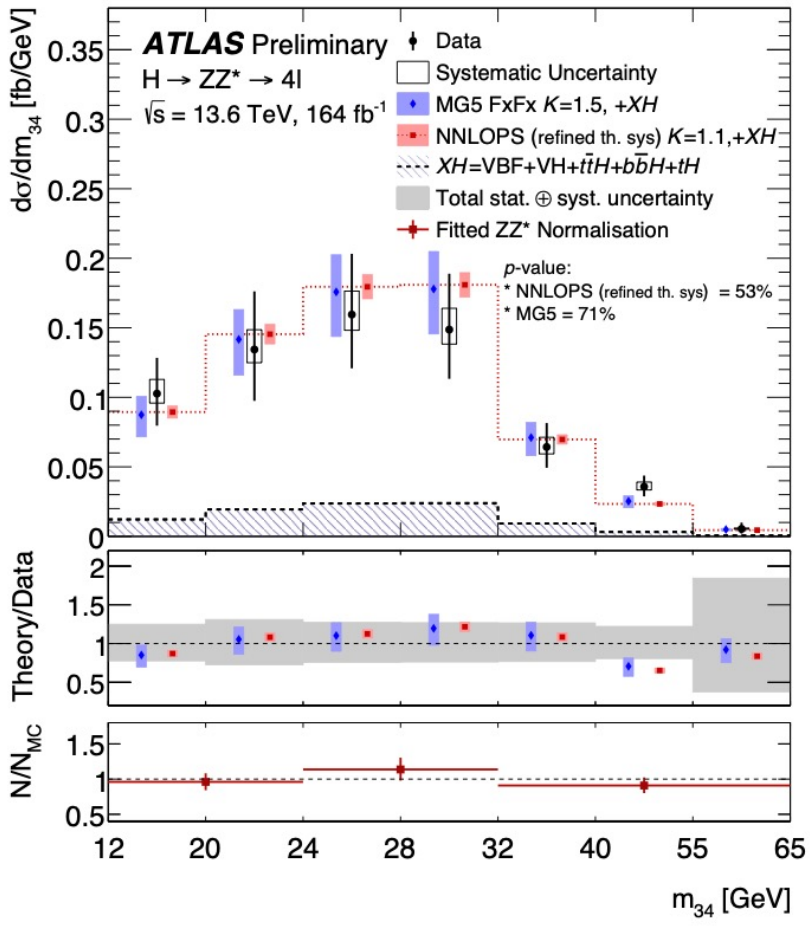

Run3 H4l

ATLAS-CONF-2026-003

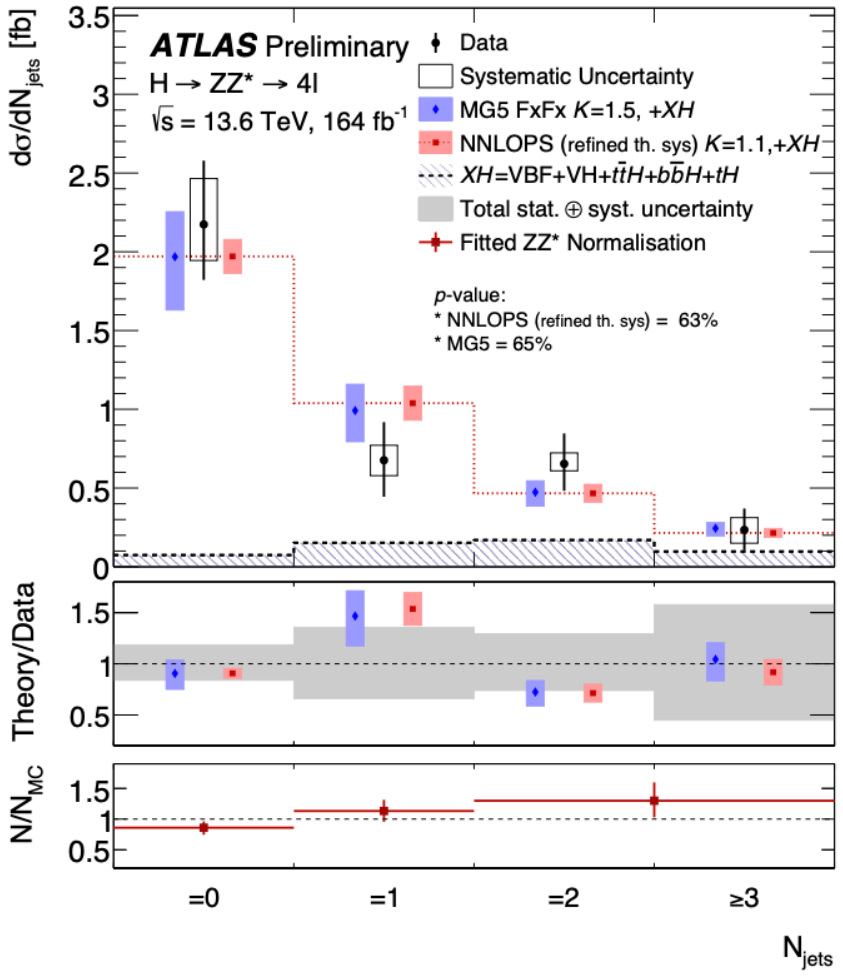

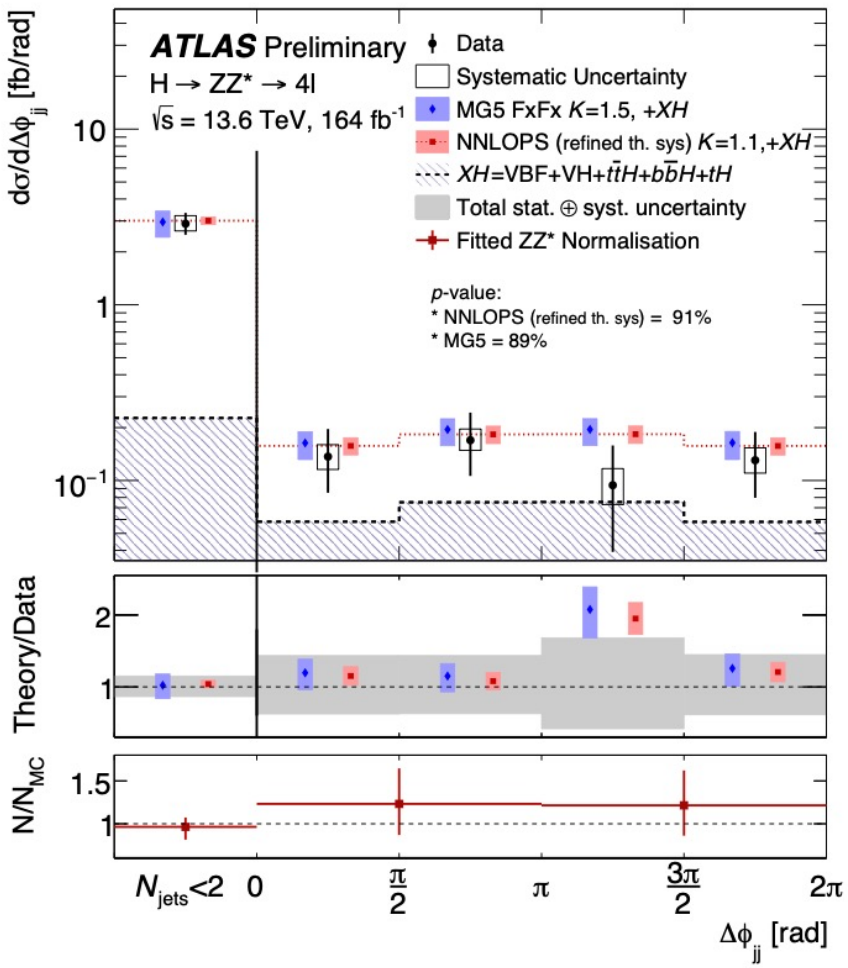

Run3 H4l

ATLAS-CONF-2026-003

Limits on the new physics scale Λ (1D fit)

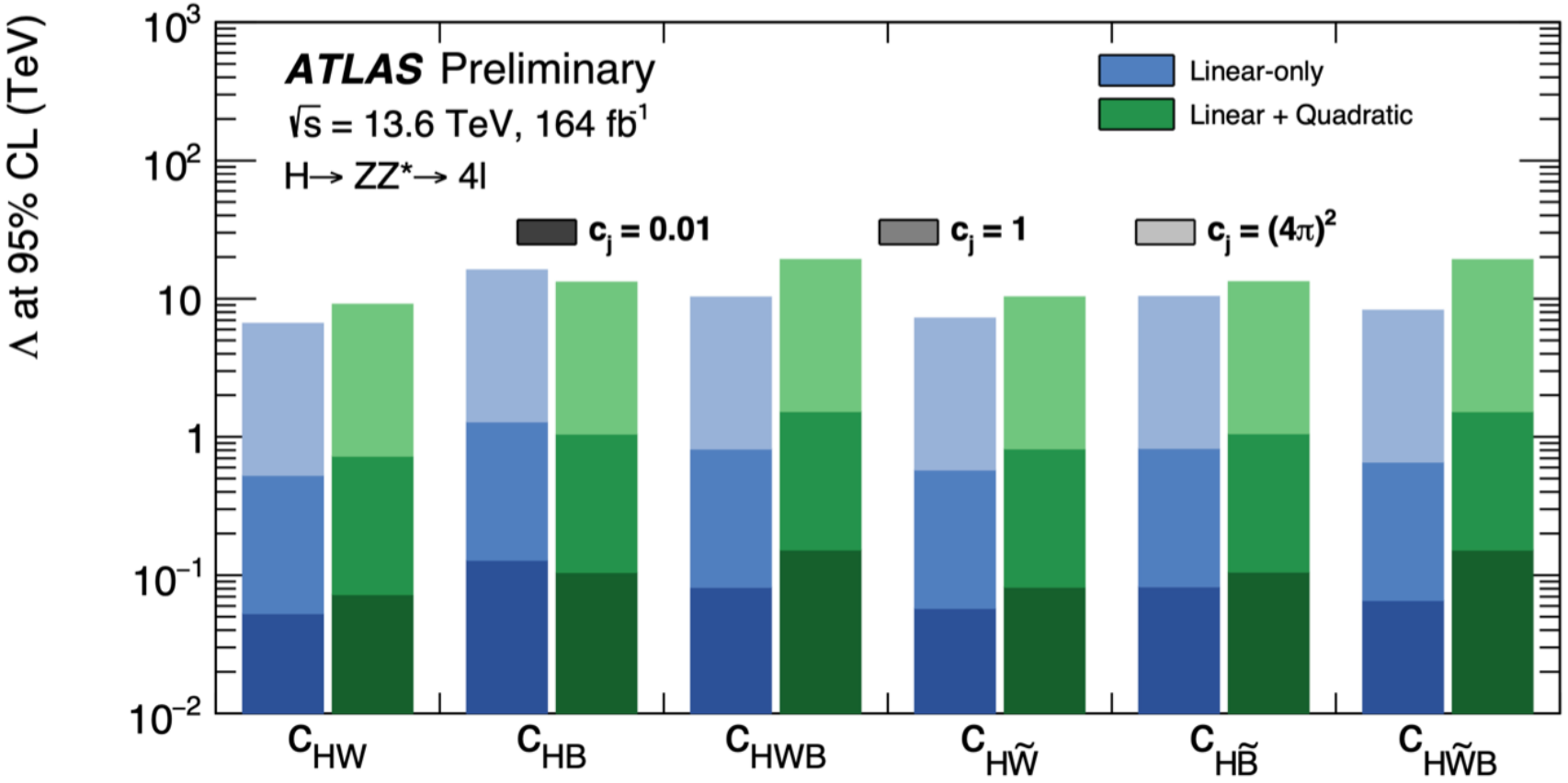

κ_λ

H+HH combination

PLB 843 (2023) 137745

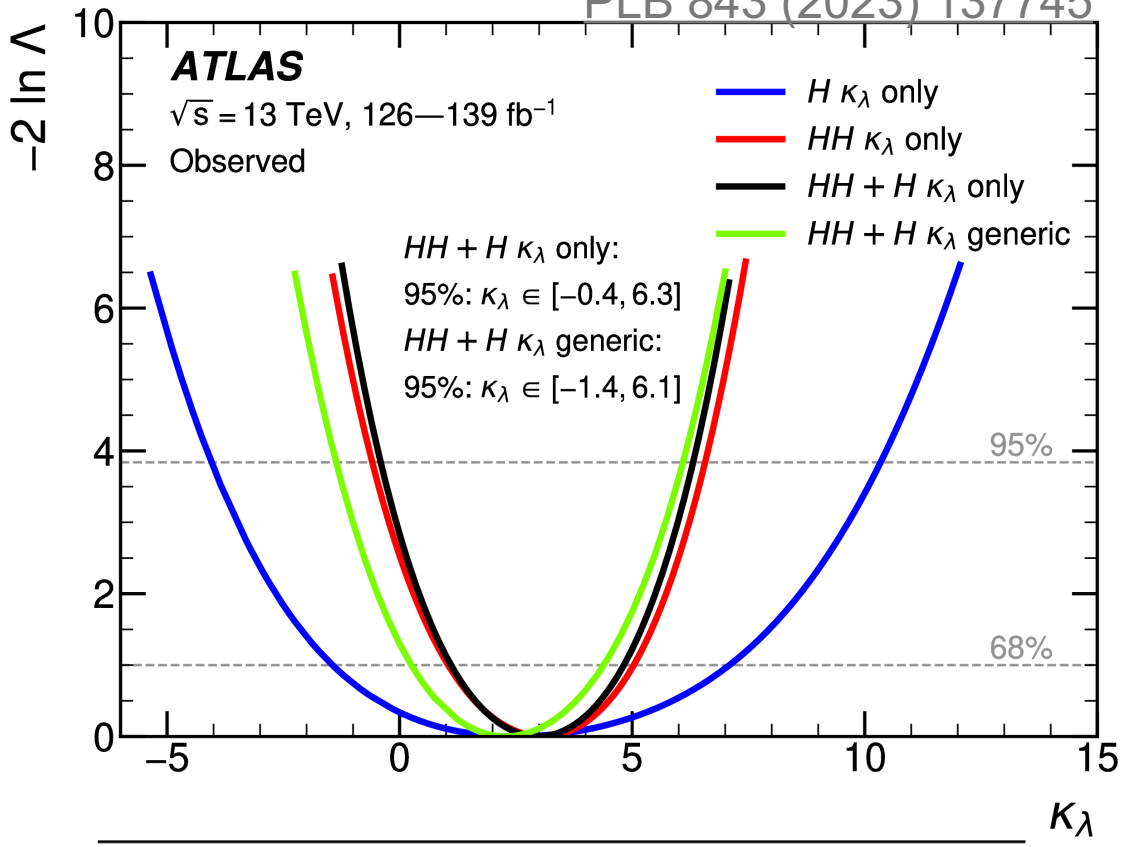

Channel	Integrated luminosity [fb^{-1}]	Ref.
$HH \to b\bar{b}\gamma\gamma$	139	[17]
$HH \to b\bar{b}\tau^+\tau^-$	139	[18]
$HH \to b\bar{b}b\bar{b}$	126	[19]

HH combination

PRL 133 (2024) 101801

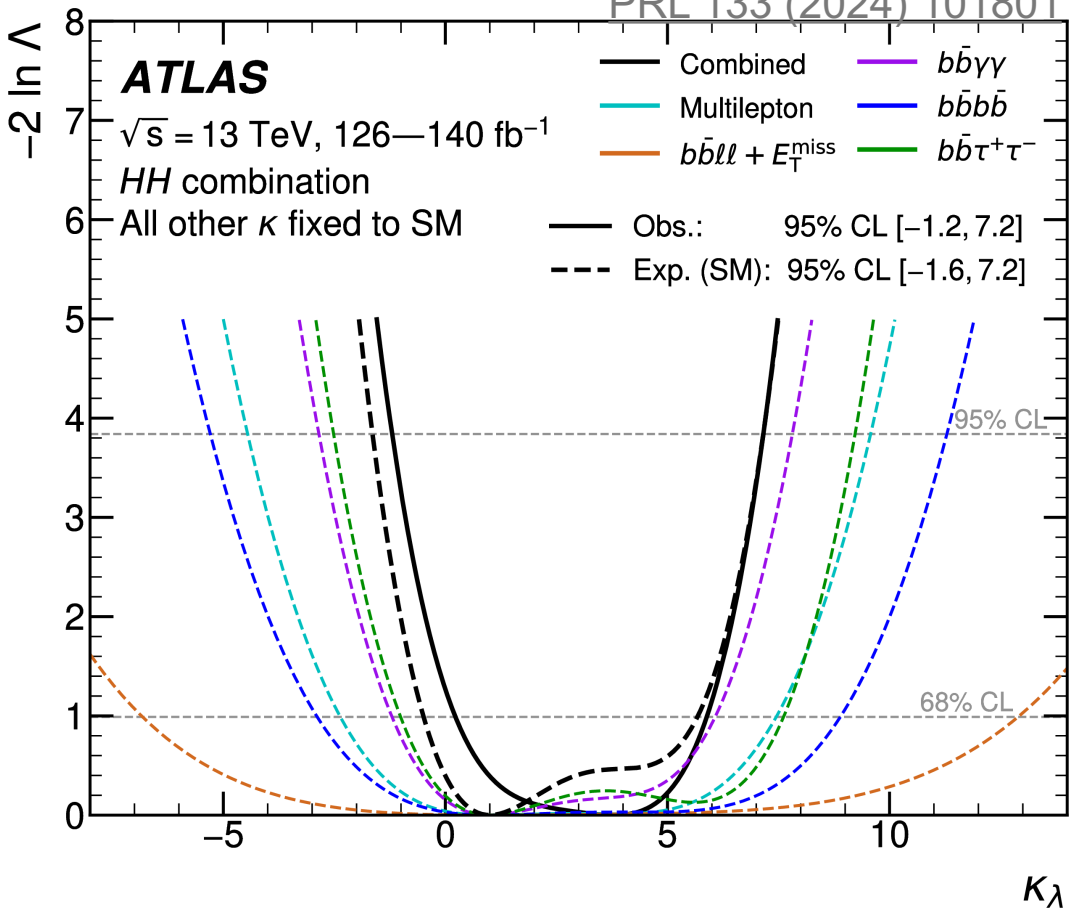

Boosted All-Had Hbb

HIGP-2024-01

- Exploiting full Run 2 (140 fb^{-1}) and part of Run 3 (2022-24, 161 fb^{-1}) datasets
- Event selection
  - At least one large-R jet with pT >450 & m>60 GeV
  - At least 2 large-R jets with pT >200 GeV
  - Tagging of Hbb candidate based on GN2X tagger
- Categorisation into signal (SR) & control/validation regions (C/VR) based on candidate requirements
  - 2.5% of anti-tagged events used for CR to constrain bkg shape
  - Rest (VR) divided into hundreds of SR stats-equivalent samples (slices) used for injection studies
- Signal region definitions and reco-pT range
  - 12 SR & 12 CR from:
  - 3 jet pT bins: [450,650], [650,1e3] GeV, >1 TeV
  - Lead(SRL) & Sub-Lead(SRS) categories

GN2X tagging decision		Jet's assigned region	
Leading jet	Subleading jet	Leading jet	Subleading jet
Pass	Pass	SRL	–
Pass	Fail	SRL	CRS/VRS
Fail	Pass	CRL/VRL	SRS
Fail	Fail	CRL/VRL	CRS/VRS

Boosted All-Had Hbb: Background

HIGP-2024-01

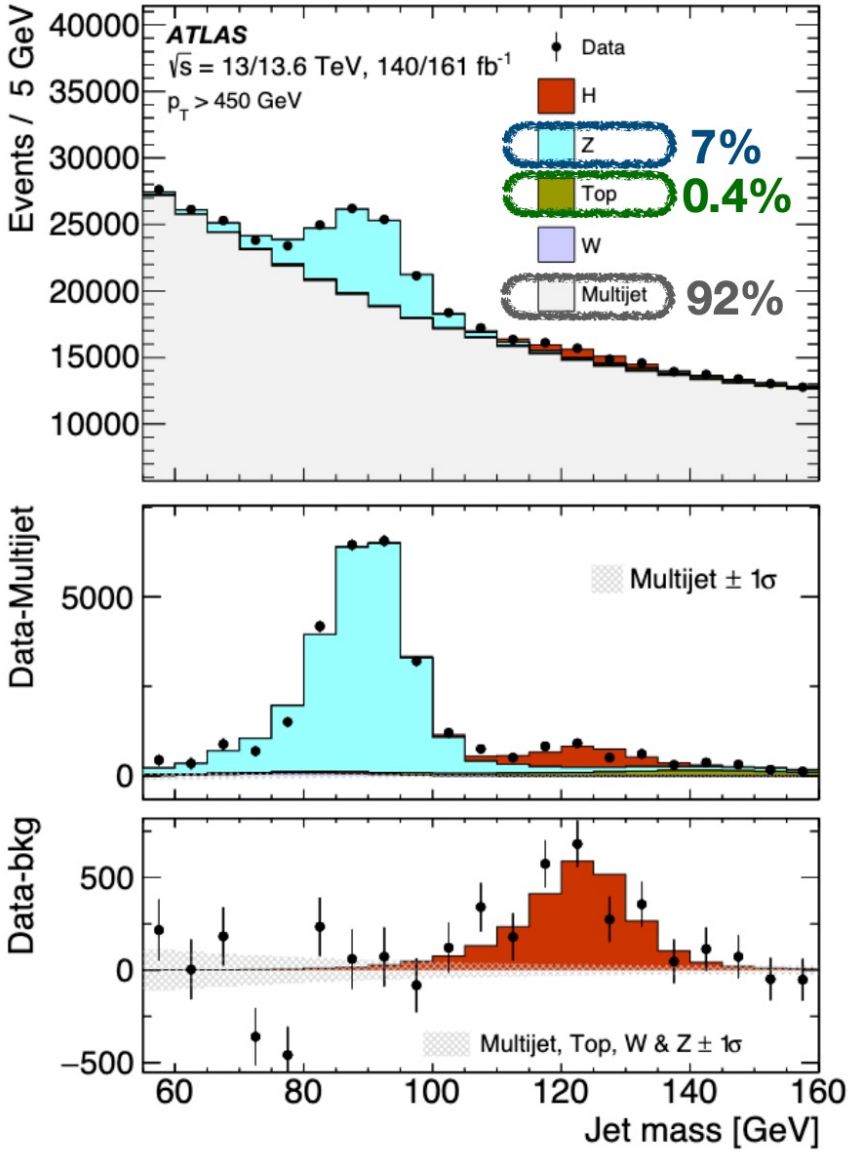

- QCD multi-jet production is by far (>90%) the largest background
  - Modelled by fitting a smooth function constrained by CR
- W/Z+j: shape from Sherpa 2.2.14(NLO QCD+NLO EW)
  - >99% is Zbb after tagging
  - Fully floating (standard candle)
- ttbar: shape from Powheg+Pythia8
  - Normalization from dedicated control region (CRttbar)
- 0.4% of SRs: small, ~as much as Higgs, and flattish contribution

Boosted All-Had Hbb: Background

HIGP-2024-01

- Data-driven modelling of main background through exponential polynomial of order N
- Additional multiplicative "transfer function" of order M applied in CR to describe possible SR-to-CR differences (flavour composition, kinematics, etc…) in QCD M spectrum
  - Optimal order of functions determined in injection tests based on μ pulls & lineaity

$$f_N(x|\vec{\phi}) = \phi_0 \exp\left(\sum_{i=1}^{N} \phi_i x^i\right) \qquad t_M(x|\vec{\psi}) = 1 + \sum_{j=1}^{M} \psi_j x^j$$

$x = (m_J - 140)\text{GeV}/70\text{GeV}$ N=3,4,5; M=1,2

- Data stats limits Higgs sensitivity in two ways: QCD normalization & mass shape
- Anti-tagged jets allow us to constrain shape (10/400=2.5% of tot) & validate fit
- **Simultaneous SR+CR fit** brings:
  - Improved Higgs stats accuracy
  - Reduction of correlations with syst uncertainties
- Rest of anti-tagged jets (VR) used to define N,M: **N=4, M=2**

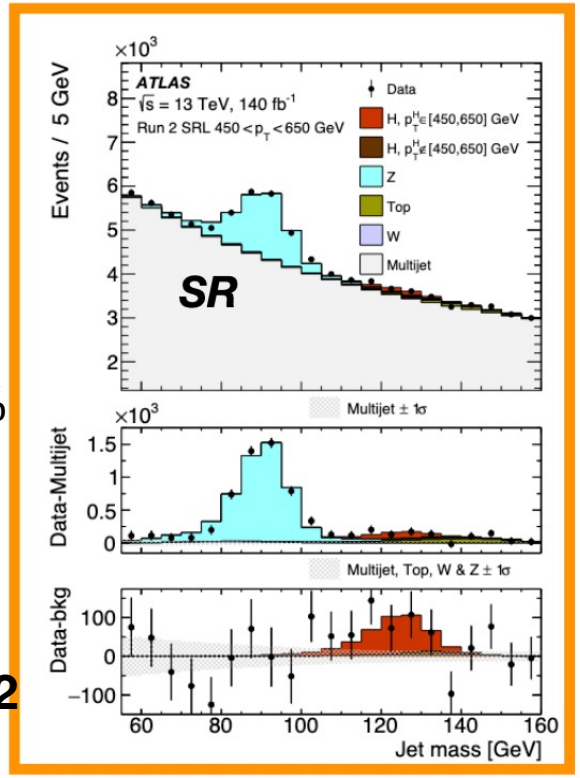

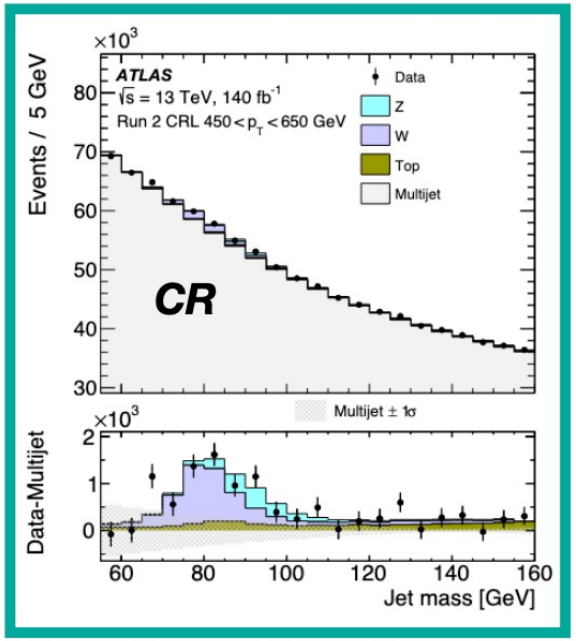

Boosted All-Had Hbb

HIGP-2024-01

- Significant presence of Higgs signal above 450 GeV
  - First evidence, 3.8(2.5)σ observed(expected)
- Improvement by factor ~10 wrt previous ATLAS result
  - Major improvement in tagging, followed by regression and simultaneous SR+CR fit

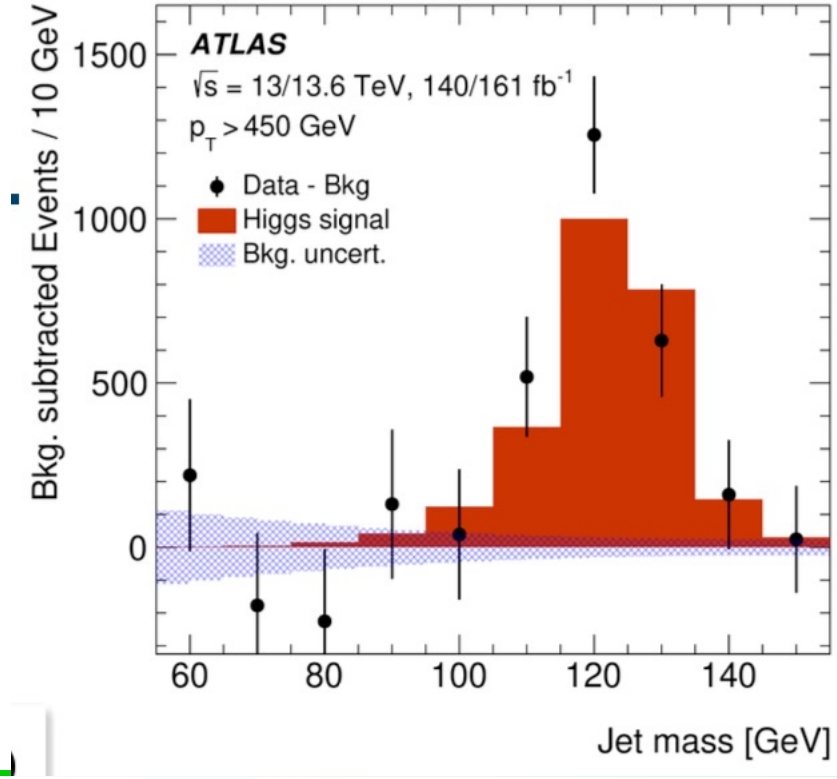

$$\mu_H = 1.53 \pm 0.27\,(\text{stat.})\,^{+0.33}_{-0.27}\,(\text{syst.})\,\pm 0.17\,(\text{theo.})$$

Boosted All-Had Hbb: p_T^H-differential Results

- Differential cross-section measurements in 3 pTH bins: [450,650], [650,1000] & >1000 GeV
  - **Most precise determination to date of Higgs boson production at high transverse momentum**
- Results enabled by advances in transformer-based jet reconstruction & simultaneous fit strategy that determines the multijet background from data

HIGP-2024-01

Run 2/3 cross-sections

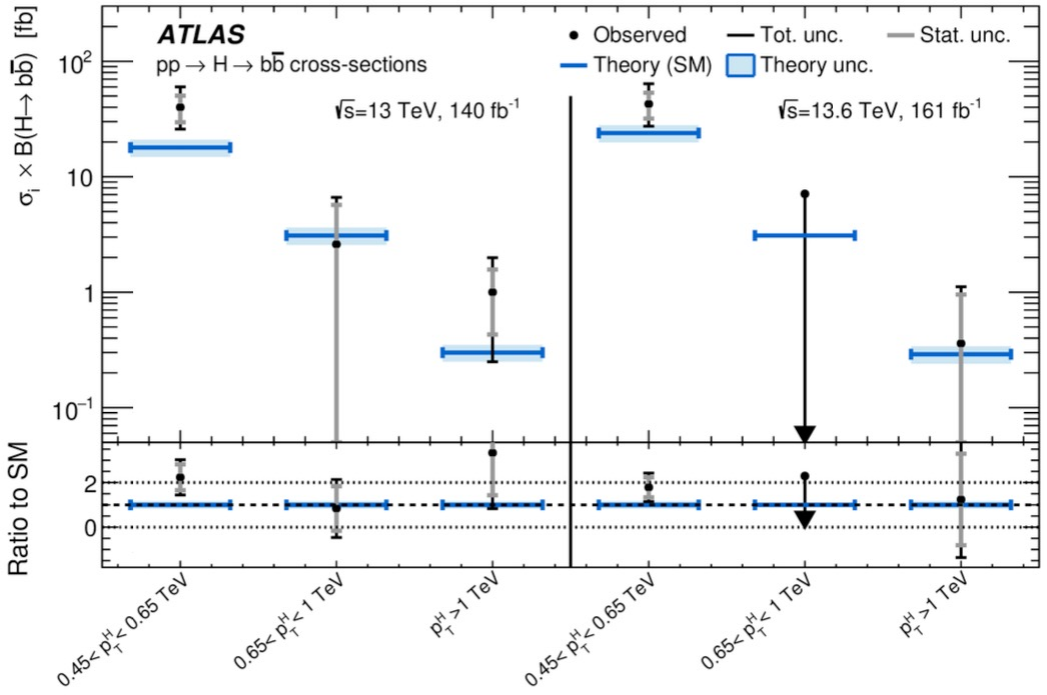

Combined Run 2+3 signal strengths

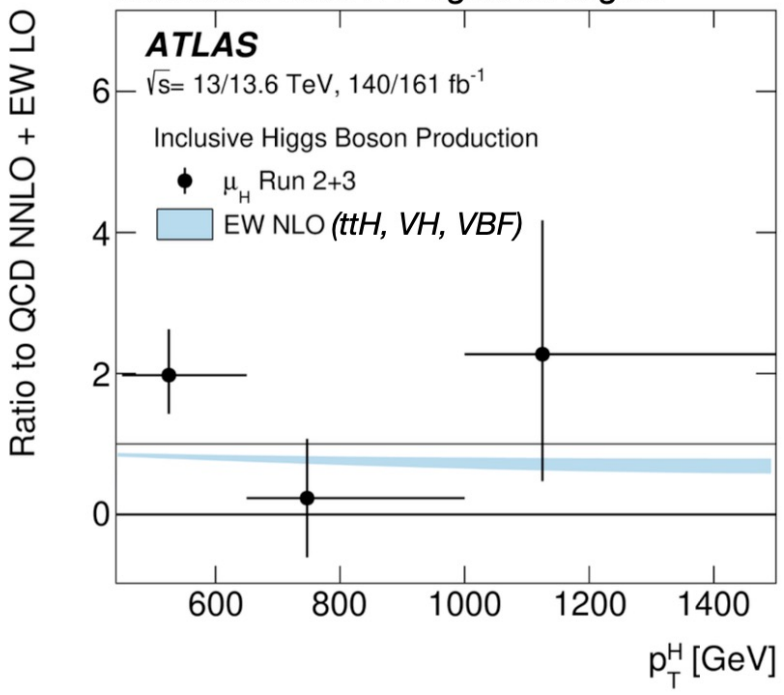

Run2 $tH(\tau\tau)$

ATLAS-CONF-2026-002

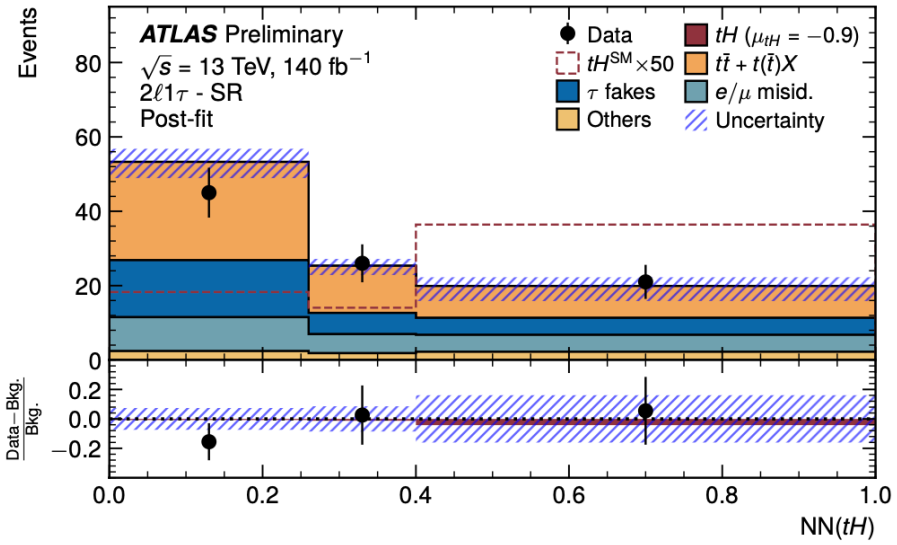

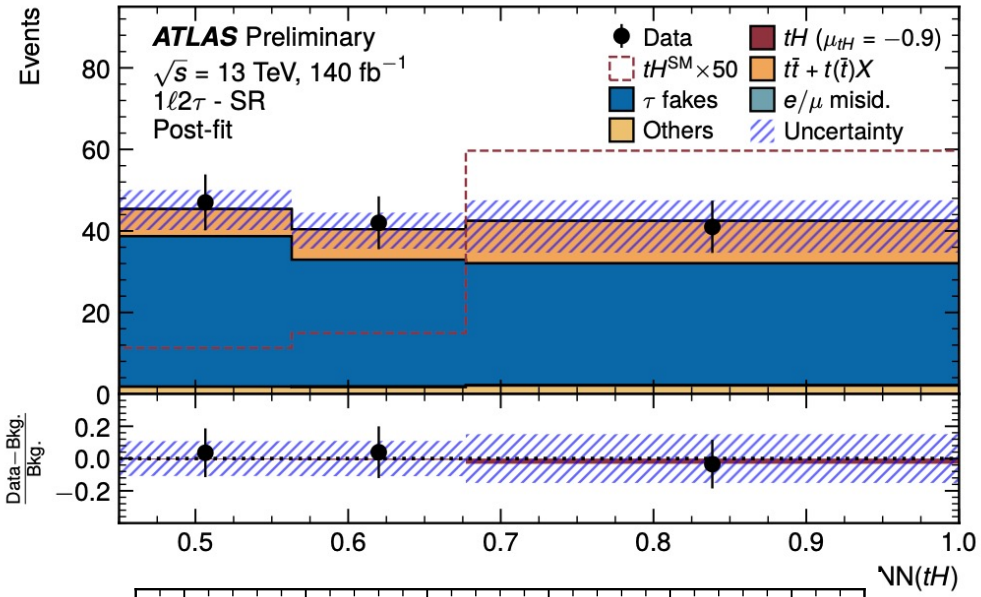

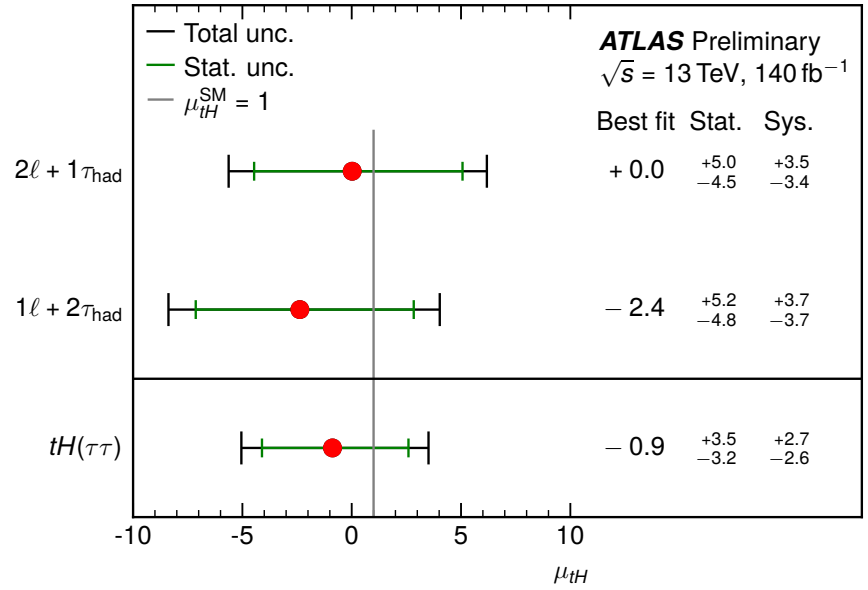

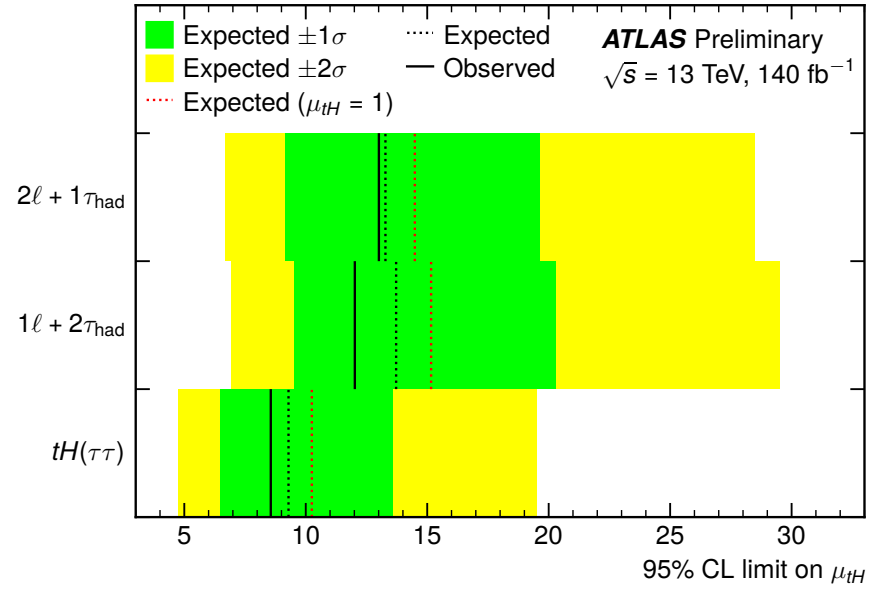

Obs. (exp) upper limit: 8.6 (9.3)

Run2 tH combination

ATLAS-CONF-2026-002

$H \to \gamma\gamma$ (ttH and tH) coupling measurement
JHEP 07 (2023) 088

tH (bb / ML)
JHEP 10 (2025) 093

tH ($\tau\tau$)

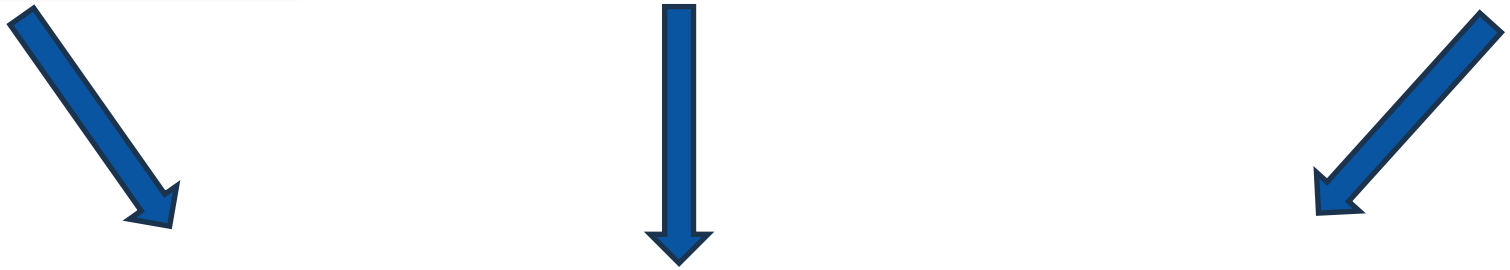

Run2 tH combination

Run2 tH combination

ATLAS-CONF-2026-002

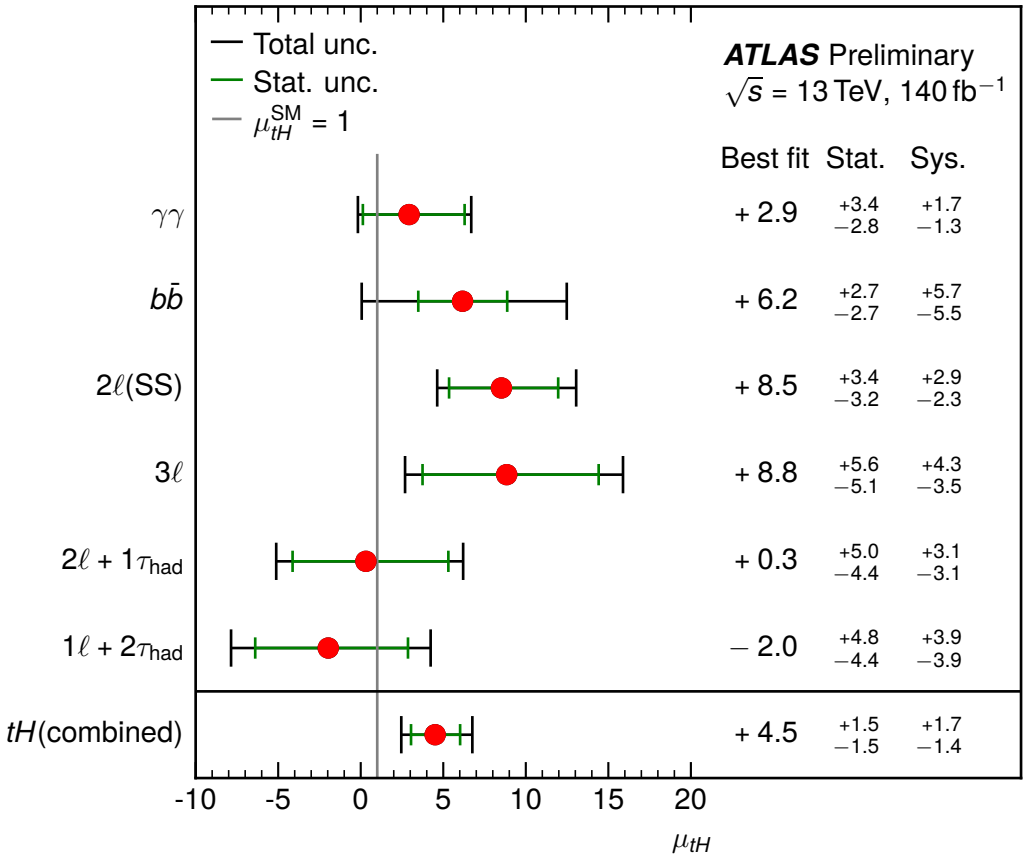

Obs. (exp) upper limit: 8.5 (3.9)

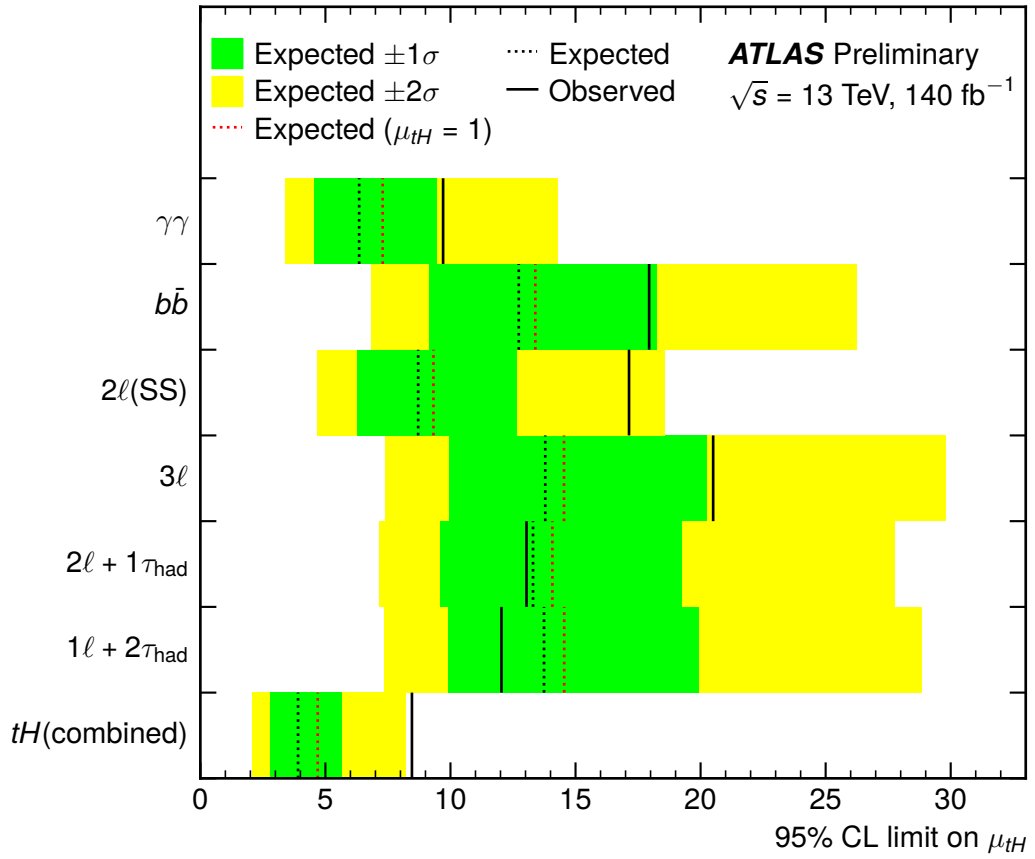

Individual results derived by floating μ_{tH} of each input channel simultaneously (correlated unc. introduce small changes w.r.t. individual fits)